Double Proximity Effect in Lateral S-NF-S Junctions

Bachelor Thesis

Andrea Peña

A thesis presented for the degree of Bachelor in Physics

Supervisors: Prof. J.Aarts and Mr.S.Voltan
2nd Reader: Dr. M.Allan
Supervisor of home university: Dr. J.Urrestilla
Leiden Institute of Physics(LION)
Leiden University
July 6, 2015

Double Proximity Effect in Lateral S-NF-S Junctions

Andrea Peña

Abstract

The Proximity effect in planar Nb-(Cu/Co)-Nb Josephson junctions, which have a Cu/Co bilayer as a weak link, is investigated in order to analyze the influence of a ferromagnet on the superconducting correlations induced into the normal metal. The different behaviors of S-N-S junctions with thicknesses of 50 nm in both Cu and Nb layers, and S-(N/F)-S junctions with 10 nm of Co and 50 nm of Cu and Nb are studied. A dramatic suppression of the Josephson critical current is observed in the junctions where the intermediate spacer between the two superconductors is a hybrid structure made by a normal metal and a ferromagnet. We believe that the observed behaviour is caused by the influence of the exchange interaction from the ferromagnet on the superconducting correlations of the electrons and holes in the weak link. This is in agreement with the length scale of the superconducting correlations being comparable to or even larger than the thickness of the Cu/Co bilayer.

Contents

Chapter 1

Introduction

The Josephson effect is one of the most relevant and fascinating quantum macroscopic effect in the field of condensate matter physics. Since 1962, when it was first described by Brian D. Josephson[1], there has been a lot of research around the Josephson junctions.

Not only most of the active superconducting devices use Josephson junctions, but also they are considered to be the basic building blocks of these devices. They have been used for a variety of applications. One of the most important is the Superconducting Quantum Interference Device (SQUID), which is the most sensitive sensor of magnetic field with a resolution close to the quantum limit.

In Superconductor-Normal metal-Superconductor (S-N-S) junctions, the phenomenon responsible for the Josephson effect is the so called proximity effect. This occurs at Superconductor-Normal interfaces and implies that the superconducting properties are induced into the normal metal within a certain length scale.

The proximity effect in S-N-S Josephson junctions has long been studied and its properties are well-known. However, it is still not clear how placing a ferromagnet next to the normal metal affects this proximity effect. The ferromagnet changes the properties of the proximity effect in the adjacent normal metal; this new effect takes the name of Double proximity effect[2].

The goal of this thesis is to investigate the proximity Effect in planar Josephson junctions, and to investigate the effects of placing a ferromagnet next to the normal metal.

We want to fully characterize the S-N-S Josephson junction, figure 1.1. Our motivation for using planar Josephson junctions, and not classical sand-

wich type junctions, is that they have the advantage of providing direct access to the superconducting correlations in the normal metal and this, in terms of future applications, is much more practical.

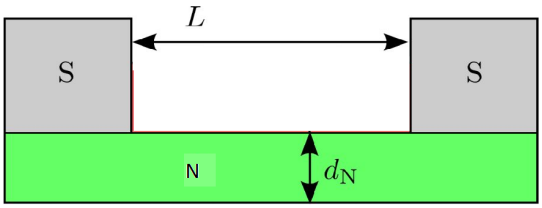

Fig. 1.1. Planar S-N-S Josephson Junction. Two superconductors are coupled by a normal metal of length L and thickness d_N.

In order to characterize S-N-S structures, it is vital to have a good insight into the relation between the critical current and temperature. That is, how the increase of the temperature changes the properties of the junction.

Furthermore, it would be of great practical importance to know how the different parameters of the junction, in particular the length, affect the Josephson effect. How does the critical current of the junction change? What is the maximum lenght of the junction above which the proximity effect is supressed and, hence, a supercurrent is not induced into the normal metal any more?

Once we fully understand the S-N-S junctions, we could be able to analyze the proximity effect in planar Josephson junctions where the intermediate spacer between the two superconductors is a hybrid structure made by a normal metal and a ferromagnet. In the figure 1.2 can be seen this type of juncion can be seen.

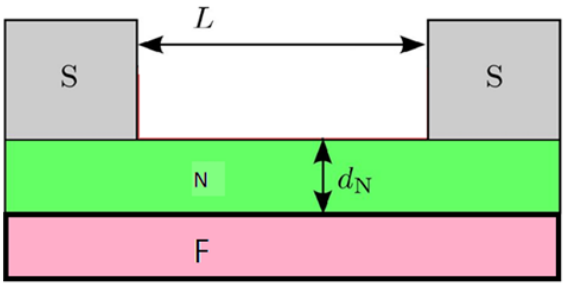

Fig. 1.2. Planar S-F/N-S Josephson Junction. Two superconductors are coupled by a bilayer of normal metal and a ferromagnet. The length is L and the thickness of the normal metal is d_N.

In S-N/F-S, which stands for Superconductor-Normal metal/Ferromagnet-Superconductor, junctions, the proximity effect induced into the weak link is affected by the exchange interaction of the ferromagnet.

Intriguing questions are raised by the study of S-F/N-S junctions: how does the ferromagnet influence the proximity effect induced into the adjacent normal metal? What is the length of the junction at which the superconductivity is completely suppressed? Furthermore, even if we have a thick layer of normal metal, would the thin layer of ferromagnt still affect the proximity effect? It would be interesting and, at the same time, non-intuitive, to see any strong influence using a thick layer of normal metal. Measuring such devices and trying to answer these questions can lead to a better insight into the physics of the proximity effect and, in general, of the interaction between ferromagnetism and superconductivity.

This thesis was done during an exchange program (ERASMUS) in the University of Leiden (The Netherlands).

Chapter 2

Theoretical background

2.1 Superconductivity and Proximity effect

Superconductivity is a physical phenomenon which involves the complete suppression of the electrical resistance and the expulsion of magnetic fields. This phenomenon occurs in certain materials, when they are cooled below a characteristic critical temperature.

Let us analyze briefly the main characteristics of the superconductors.

When materials are in the superconducting state, they repel magnetic fields as expected for a perfect conductor; however, Walther Meissner and Robert Ochsenfeld found in 1933 [3] that the magnetic field was expelled from the superconductor during the transition from the normal to the superconducting state. So, instead of trapping a magnetic field inside, which is, according to classical physics, what a perfect conductor could do, in the superconducting case, the magnetic fields generate superconducting Foucault currents (circular electric currents) that create an opposing field of exactly the same absolute value of the applied field. This repels the flux and makes the material a perfect diamagnet. Such behavior is sketched in the Fig. 2.1.1.

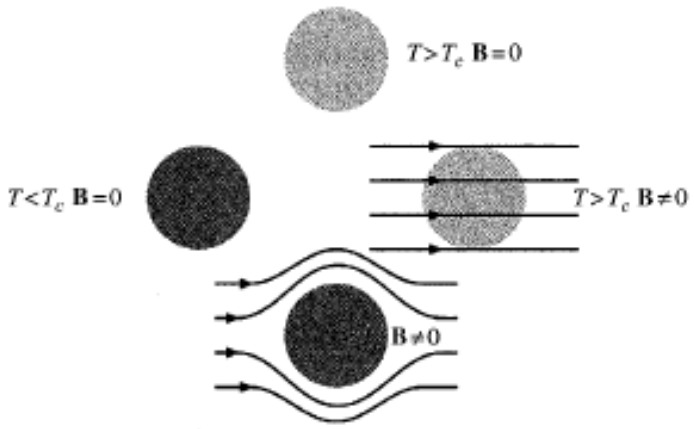

Fig. 2.1.1. If a sample initially at high temperature and in zero magnetic field (top) is first cooled (left) and then placed in a magnetic field (bottom), then the magnetic field cannot enter in the material. This is a consequence of zero resistivity: $\rho = 0$. On the other hand, a normal sample (top) can be first placed in a magnetic field (right) and then cooled (bottom). In this case the magnetic field is expelled from the system. This property that characterizes a superconductor is called the Meissner-Ochsenfeld effect. This figure is taken from the reference [4].

Every superconductor can be characterized by 3 parameters: critical temperature T_c , critical current I_c and critical magnetic field H_c .These three properties are related to each other. For example, cooling down a material below its critical temperature at zero field, would imply the abrupt vanishing of the resistance, as it can be seen in the figure 2.1.2, in which the resistivity of a superconducting material versus the temperature is plotted.

Normal state can be restored by applying a sufficiently strong current (larger than the critical one) or putting it in a sufficiently strong field (larger than the critical magnetic field).

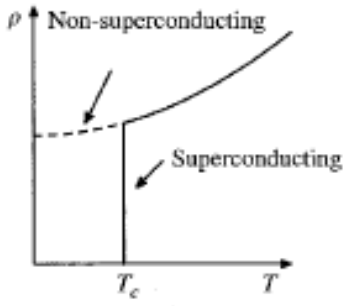

Fig. 2.1.2. Resistivity of a typical metal as a function of temperature. If it is a non-superconducting metal the resistivity approaches a finite value at zero temperature, while for superconductors all signs of resistance disappear suddenly below a certain temperature. This figure is taken from the reference [4].

As was mentioned before, a weak magnetic field cannot penetrate in a superconductor, but when the magnetic field increases enough the superconductivity breaks down.

Accordingly to how a superconductor behaves in a presence of a magnetic field, it can be classified into two types of superconductors: Type I and Type II.

For Type I superconductors, just after the applied magnetic field exceeds the critical magnetic field, the superconductivity is abruptly destroyed.

Type II superconductors, instead, exhibit two critical magnetic fields: the lower one, H_{c1} , which occurs when magnetic flux vortices penetrate the material; however, it still remains superconducting in most of the regions except from these microscopic vortices; and the upper one, H_{c2}, which occurs when the normal state is completely recovered. So, Type-II superconductors usually exist in a mixed state of normal and superconducting regions.

The differences between the 2 types of superconductors can be appreciated in figure 2.1.3, where the magnetic field is plotted as a function of temperature.

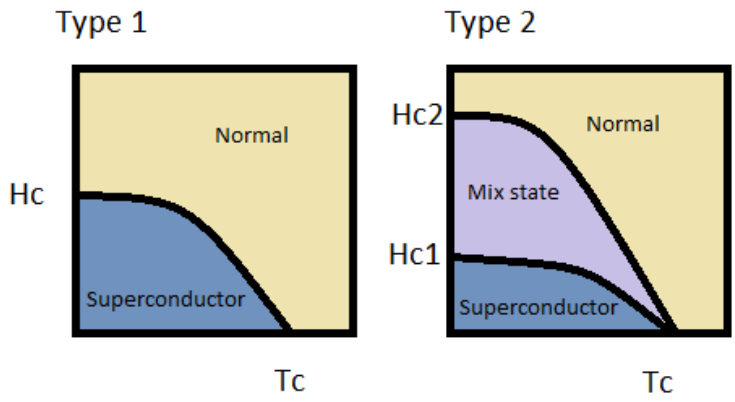

Fig. 2.1.3. Magnetic field versus temperature phase diagram of Type I and Type II superconductors.

Although there were a lot of attempts to describe the phenomena related to the electrodynamics of superconductors, the first successful description was given by the London theory (1935). Nowadays, one of the most important theories in order to describe superconductivity is the Ginzburg-Landau theory (1950). It is a phenomenological theory, but in this case, it takes into account the quantum effects by introducing a wave function, also called the order parameter. The GL theory is valid only near the critical temperature of the superconductor, because it is based on the theory of phase transitions.

The superconducting state and the normal metalic state are considered to be different phases of matter. Hence, in this model superconductivity is analyzed from the point of view of the thermodynamics of phase transitions. We therefore define an order parameter, ψ, which characterizes the superconducting state. In the framework of the GL theory, the so called proximity effect can be described. This occurs when a superconductor is placed in contact with a Normal metal (non-superconductor). In the normal metallic state (above the critical temperature T_c of the superconductor) it is zero, while in the superconducting state (below T_c) it is non-zero.

$$\Psi = 0,\ T > T_c$$
$$\Psi \neq 0,\ T < T_c$$

Superconducting properties can be induced into the normal metal, but only near the interface on a small length scale, usually characterized as ξ_n.

This means that the wave function which describes the superconducting state, can actually survive for a small length in the normal metal, until it completely becomes zero, as it can be seen in figure 2.1.4. This effect is called the proximity Effect.

For normal metals, ξ_n, the normal penetration depth, is of the order of micrometers. It is given by the following equation:

$$\xi_n = \sqrt{\frac{\hbar D}{k_B T_c}} \tag{2.1}$$

where the D is the diffusion coefficient of the normal metal and T_c is the critical temperature of the superconductor.

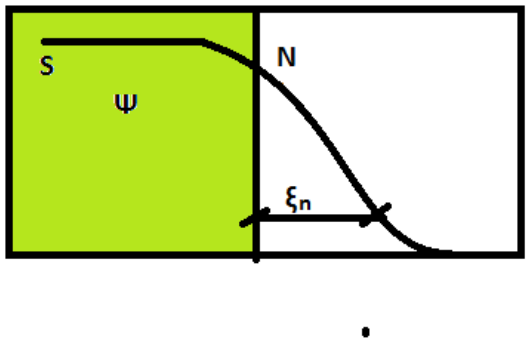

Fig. 2.1.4. Proximity effect in SN structure. It can be seen how the order parameter survives over a length scale, denoted as ξ_n, which is called the normal penetration depth.

2.2 Josephson Junction

The so-called Josephson effect occurs in hybrid structures which consist of two superconductors that are connected via a weak link region (dielectric material, normal metal, constriction). The Josephson effect is an example of a macroscopic quantum phenomenon.

The Josephson junction behaves differently when the applied current is either above a certain characteristic current or below it. Let us analyze these

two behaviors:

The first one, called the DC Josephson Effect, occurs when a sufficiently small current passes through the Josephson junction without dissipation; meaning the junction does not show any resistance at all. This implies that, when such a current passes through the weak link, no voltage is generated across the junction. The current will be as follows:

$$I = I_c sin(\phi) \tag{2.2}$$

where ϕ is the phase difference across the weak link and I_c is the maximum dissipation-free current through the junction, often referred as the Josephson critical current.

The second one is called AC Josephson effect. It happens when the I exceeds the I_c, and this fact will cause a voltage V appearing across the junction.

$$V = \frac{\hbar}{2e}\frac{\partial \phi}{\partial t} \tag{2.3}$$

And hence,

$$I = I_c sin(\phi) + \frac{\hbar}{2eR}\frac{\partial \phi}{\partial t} \tag{2.4}$$

where R is the normal-state resistance of the junction.

You can see in the purple curve of figure 2.2.1 these two behaviors of a Josephson junction.

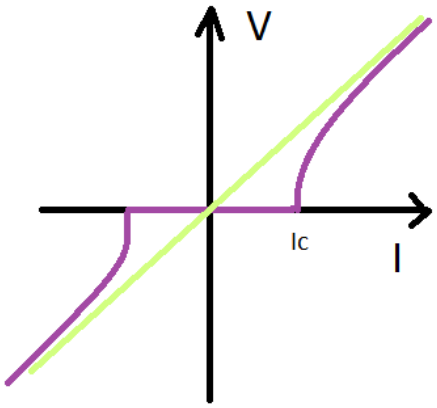

Fig. 2.2.1. Voltage versus current curves. In purple the characteristic V-I curve of a Josephson junction. The green straight line shows the Ohmic behaviour of a normal resistance.

We now focus our attention on the response of the critical current to an external magnetic field. The application of an external magnetic field parallel to the plane of the junction will change the distribution of the current. When the Josephson junction is in a magnetic field, the phase of the junction is not the same along the width of its barrier any more. The flux will make the phase to vary spatially, which results in a new distribution of the supercurrent.

The maximum supercurrent through a Josephson junction versus the external magnetic field parallel to the plane of the junction will be given by (see section 4.4 in reference [5] for the mathematical developing of this expression):

$$I_{max} = I_c \left| \frac{sin(\frac{\pi\Phi}{\Phi_0})}{\frac{\pi\Phi}{\Phi_0}} \right| \tag{2.5}$$

where Φ is the total magnetic flux trough the Josephson Junction and Φ_0 is the quantum flux, which has a value of $\frac{\hbar}{2e} = 2.07 \times 10^{-15}$ Wb (Deaver and Fairtbank were the first to observe the phenomenon of flux quantization, see reference [6])

Plotting critical current vs. applied magnetic field produces a so-called Fraunhofer pattern, as it can be seen in the figure 2.2.2.

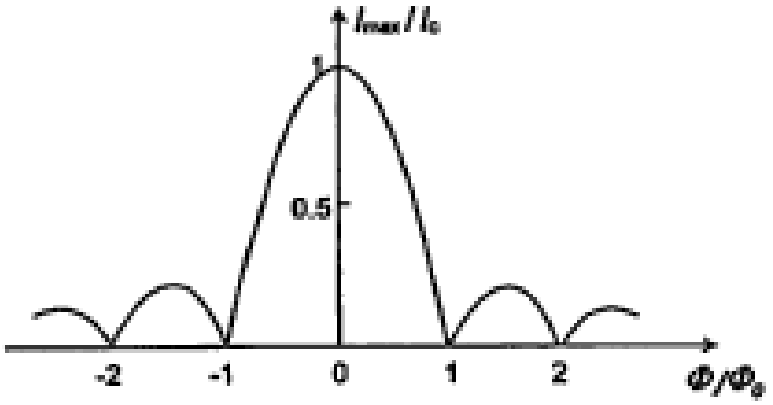

Fig. 2.2.2 The critical current of a Josephson junction as a function of the applied magnetic flux Φ in units of the flux quantum Φ_0. This figure is taken from reference [5].

The minimun points occur when there are integer values of Φ_0, because there is an equal amount of current in both directions. The maximum points occur at half integer values of Φ_0. Note that the maximum amplitude is reduced as the oscillations become smaller.

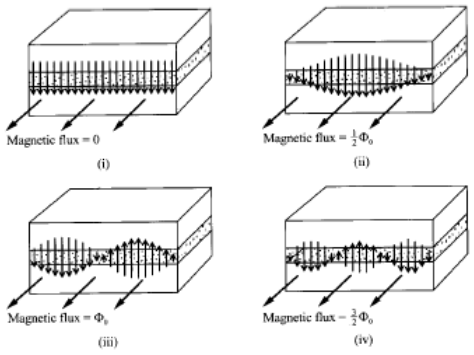

Fig. 2.2.3. Spatial distribution of the supercurrent in a Josephson junction for diferent values of magnetic flux. One can see that at the minima in the sinc function in Figure 2.2.2 that there is an equal amount of current

in both directions. For half integer values of ϕ_0 the net-current flow is in one direction but its magnitude is reduced as more oscillations traverse the junction. This figure is adapted from Reference [7].

2.3 BCS theory and Andreev reflection

Until now we have explained Superconductivity and the proximity Effect from a macroscopical point of view, let us now do it from the microscopical one.

In 1957 Bardeen Cooper and Schrieffer published for the first time a truly microscopic theory which explains the phenomena of superconductivity [8]. Cooper suggested the idea of bound electrons, Cooper pairs, which are formed by electrons that are near the Fermi surface. These electrons interact with each other due to small electro-phonon forces, and become pairs. The BCS theory was based on this idea.

Cooper pairs behave as bosons as their spin is an integer number. Hence, in the metal there is no fermionic distribution any more and the Pauli exclusion principle does not have to be fulfilled. At temperatures below T_c, the Cooper pairs can accumulate in the ground state and consequently, they can travel trough the material without any dissipation.

The size of the Cooper pairs is given by the superconducting coherence length, ξ_s. This length scale represents how far away are the two electrons forming the Cooper pair from each other. The interaction between these pair of electrons is not energetic; in fact, it is really weak, of the order of $10^3 eV$, and thermal energy can easily break the pairs. So only at low temperatures there are a significant number of the electrons in Cooper pairs.

The Cooper pairs in a body tend to remain in the same ground quantum state: they 'condense', and this is the responsible for the peculiar properties characteristic of a superconductor.

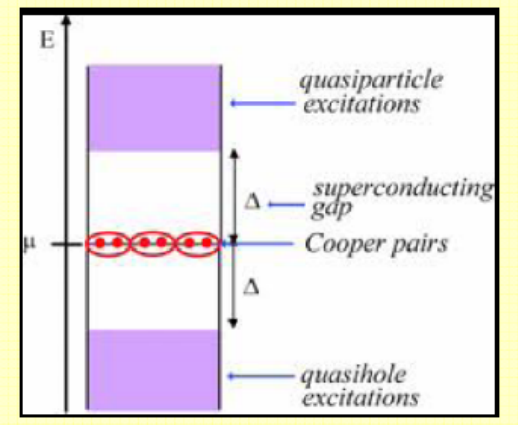

Fig. 2.3.1. The condensate is at energy ϵ_F and the quasiparticles (electrons and holes) are at $\pm\Delta$.

In conventional superconductors, the Cooper pairs are constituted by electrons that have opposite spin, forming so-called spin-singlet pairs.

The orbital wave function is type s and the spin wave function is spin singlet (total spin S=0):

$\psi = \frac{1}{\sqrt{2}}|\uparrow,\downarrow\rangle - |\uparrow,\downarrow\rangle$

However, other types of pairings are also permitted by the governing Pauli-principle.

The spin wave function is spin triplet(S=1), but in this case, the orbital wave function is a p type function.

$\psi = |\uparrow,\uparrow\rangle$

$\psi = \frac{1}{\sqrt{2}}|\uparrow,\downarrow\rangle - |\uparrow,\downarrow\rangle$

$\psi = |\downarrow,\downarrow\rangle$

As it has been said before, almost all known superconductors have singlet Cooper pairs and these are the ones which are studied in this thesis.

The microscopic model for describing the proximity effect in SN interface is called Andreev refection. In this process there is a charge-transfer, each Andreev reflection implies the transmission of 2 electrons through the superconductor, and at the same time the creation of a hole in the normal metal. The normal current, when it arrives at the interface between the normal metal and the superconductor, will become a superconducting current

in the superconductor. A schematic of the Andreev reflection can be seen in the following figure (Fig. 2.3.2):

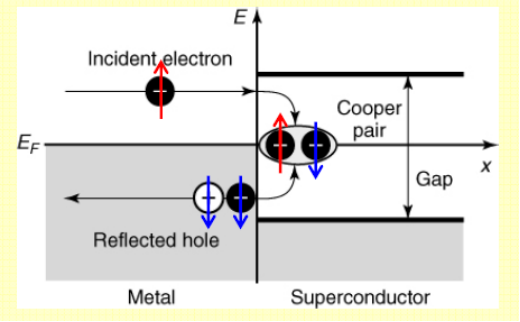

Fig. 2.3.2. The process occurs at energies less than the superconducting energy gap. The incident electron from the normal metal forms a Cooper pair in the superconductor. At the same time, the retroreflection of a hole occurs, and it has opposite spin and velocity to the incident electron, but equal momentum.

In a S-N-S interface this process leads to the transfer of Cooper pairs. This is shown is the following figure:

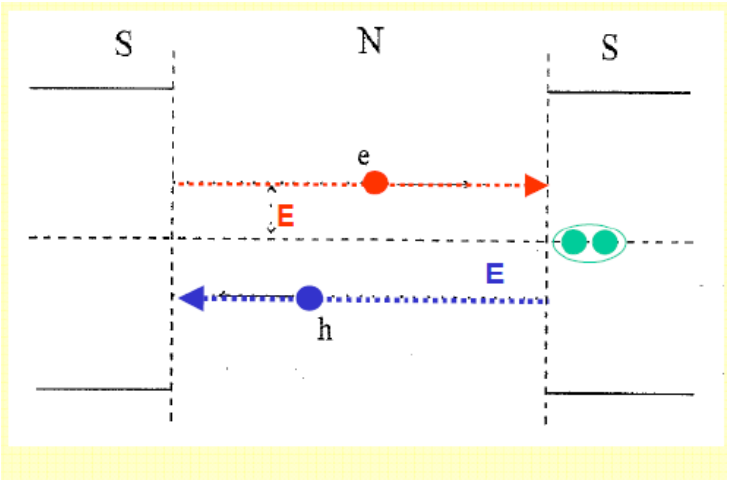

Fig. 2.3.3. S-N-S Josephson junction. Due to the Andreev reflection phenomenon a dissipationless supercurrent can be measured in the normal metal. e stands for 'electron', h for 'hole' and E represents the energy of the superconducting gap.

2.4 Ferromagnetism and Superconductivity

Ferromagnetic materials exhibit a long-range ordering phenomenon at the atomic level: the electron spins tend to line up parallel with each other in a region called a domain. In ferromagnetic materials there is a particular quantum mechanical interaction, and this interaction is the one responsible for the appearance of the long range order phenomenom, which at the same time creates the magnetic domains. Although there are thermal agitations which tend to randomize any atomic-level order, this quantum interaction characteristical of the ferromagnets, locks the magnetic moments of neighboring atoms into a rigid parallel order.

In ferromagnetic materials the parallel spin state is more stable than the antiparallel one, this is due to the exchange interaction. In this type of materials, when the electrons have parallel spins the distribution of their electric charge in the space is further apart than in the case of antiparallel spins. This means that the electrons with parallel spin have a smaller electrostatic energy, which makes them more stable.

Figure 2.4.1 shows the different atomic properties that a superconductor and a ferromagnet have.

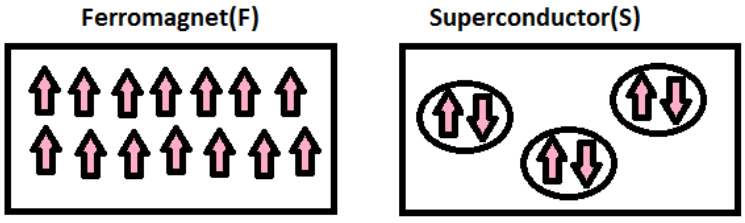

Fig. 2.4.1 Difference between ferromagnets and superconductors. In a (perfect) ferromagnet all spins are align, yielding a non-zero total magnetization. In the superconducting state, pairs of electrons form with opposite spin (singlet) resulting in zero total magnetic moment.

Let us briefly explain the difference between the proximity effect at a SN (Superconducting-Normal) interface and the one in at SF (Superconducting-Ferromagnet) interface.

In the SN system the Cooper pairs originated in the superconductors can cross the interface by the Andreev reflection, after which the Cooper pairs start to break. They slowly dephase in the normal metal, meaning that they recover the classical behavior of normal electrons. If the normal metal is now replaced with a ferromagnet, the initial situation is the same, only in this case after crossing the interface the Cooper pairs are suddenly subject to the huge exchange interaction of the ferromagnet, which causes the spins to be aligned, and is translated in a much faster dephasing.

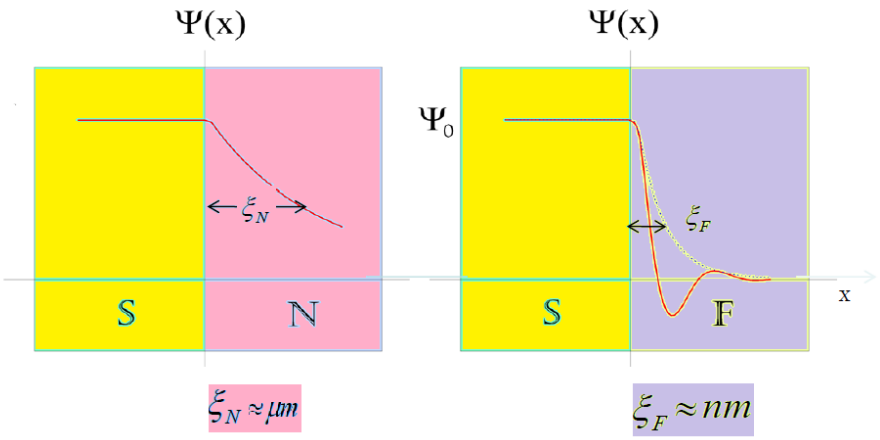

Fig. 2.4.2 Difference between a SF and SN interface. The proximity effect in the ferromagnet is weaker than in the normal metal.

As it can be seen in the figure above, the penetration depth of the ferromagnetic material is much smaller than the one of the normal metal.

The value for the ξ_F is the following:

$$\xi_F = \sqrt{\frac{\hbar D_F}{2\pi E_{ex}}} \tag{2.6}$$

being the E_{ex} the exchange energy of the ferromagnet and D_F the diffussion coefficient of the ferromagnet.

Ferromagnetism is usually considered to be incompatible with conventional superconductivity, as it destroys the singlet correlations responsible for the pairing interaction. However, it has been proven that superconductivity and ferromagnetism can actually coexist. (for example, see references [9] and [10]).

In a SF interface a singlet Cooper pair, $|\uparrow,\downarrow\rangle - |\uparrow,\downarrow\rangle$, could not survive for a long time(it is a very short ranged effect in comparison to the normal metal); but a triplet Cooper pair,$|\uparrow,\uparrow\rangle, |\downarrow,\downarrow\rangle$ could survive.

If somehow the singlet wavefunction could be converted into an equal spin triplet correlation, it would be exposed to less breaking interaction, leaving only the normal metal dephasing due to the usual electronic dispersion.

There is currently lot of research in the generation of triplets, which is a topic that is not analyzed in this thesis, but more information can be found in Reference [11] and [12], for example.

Chapter 3

Experiment

Submicron devices are fabricated step by step (film deposition, electron beam lithography and etching) and characterized with measurements at low temperatures.

Different experiments are performed using Nb-Cu-Nb (superconductor-normal metal-superconductor) junctions, in order to see the Josephson supercurrent through the weak link and hence, the quantum macroscopic effect that this would imply.

Once the S-N-S junctions are characterized and their proximity effect fully understood, 10 nm of cobalt is placed next to the copper creating S-N/F-S junctions. Differences of these two junctions are investigated in order to analyze the effect of the ferromagnet in the proximity effect.

In the following figure the structure of a Josephson junction can be seen. We work with junctions with a gap length l between 75 nm and 300 nm. The width w is 2 μm, and the thicknesses of the materials used are d_S 50 nm of Nb, d_N 50 nm of Cu and ,for the Nb-Cu/Co-Nb junctions, d_F 10 nm of Co.

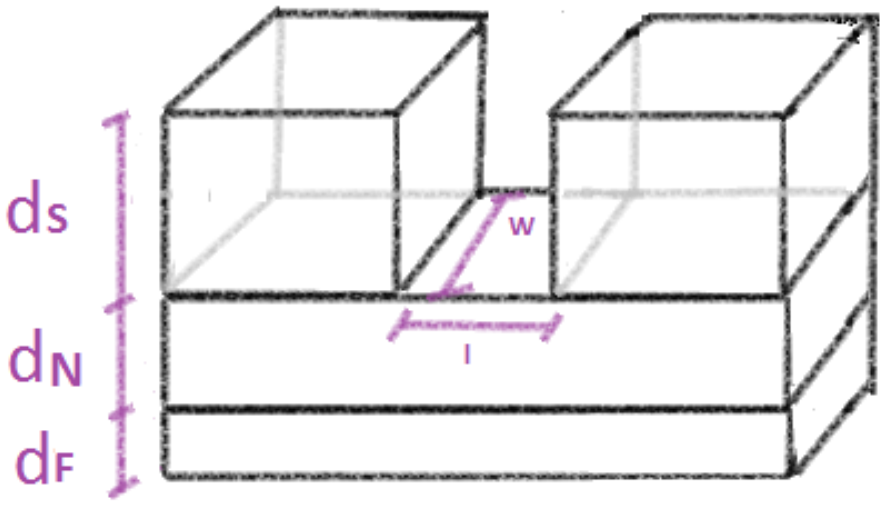

Fig. 3.1. In this figure it can be seen the S-N/F-S structure, where l is the length, w is the width and d_S, d_N and d_F is the thickness of the superconductor, the normal metal and the ferromagnet respectively.

3.1 Device Fabrication

In this section, the principal points for the fabrication of a Josephson junction are explained. In the Appendix, a detailed description of the procedure step by step can be found, with all the timing parameters, in order to provide the reader with a better understanding of the whole fabrication procedure.

For the fabrication of the Josephson junctions electron beam litography is used twice. In the first step we make the 4 contacts and the bridge of the pattern shown in figure 3.1.1. We then sputter the desired materials and after the lift-off procedure we use a second time the e-beam. In this second step, we make the gap of the josephson junction, and we etch the niobium on top of the weak link. In both of the steps of the e-beam positive resists are used. During the research we have come to the conclusion that this method is the most suitable and reliable for the fabrication of the planar junctions, as it provide us with a better control over the structures than other methods using negative resist.

Firstly, the pattern which can be seen in the figure 3.1.1 is made, (except from the small gap, the junction) in the silicon substrate, which has an area around 5 mm x 5 mm. Positive resist is used, meaning that the e-beam changes the chemical structure of the resist so that it becomes more soluble in the developer. The exposed resist is then washed away by the developer solution, and the desired pattern is left, where materials can be deposited on it.

Secondly, the materials are sputtered using the ATC-1800 sputtering system. For S-N-S junctions, 50 nm of Cu and 50 nm of Nb, and for S-N/F-S junctions 10 nm of Co, 50 nm of Cu and 50 nm of Nb. Background pressures are between 5×10^{-8} - 15×10^{-8} mBar and the sputtering presures is $6.67 \times 10^{-3} mBar$. It must be noted that a thin layer of Cu is also sputter on top of the Nb, in order to protect it.

The reason for doing this is to increase the critical temperature of the structures. The Nb is a Type II superconductor which has the highest critical temperature among the elemental superconductors. However, its superconductive properties are strongly dependent on the purity of the Nb metal. In our case, the T_c of the niobium has a value around 5 K, but when the Josephson junction is made, the critical temperature decreases to values around 2 K. One of the most probable reason for having such big decrease could be that the Nb itself gets damaged in the process. The responsible for such a low T_c could be the degassing of the resist which is placed on top of the superconductor in the second step of the e-beam. This makes really impure the niobium. In order to protect the Nb and try to keep it as pure as possible, a layer of Cu with thickness around 7 nm is placed on top of the structure. It is proved that using this layer on top, the T_c increases remarkably. In most of the next samples critical temperatures between 4.5-5 K are obtained, which provides with a much better control on the Josephson junctions.

Using acetone the resist of the sides is washed away.

In the second step of the electron beam lithography the gap for the Josephson junction is made (Fig. 3.1.2). Positive resist is used again, and after the development, both the thin layer of copper and the 50 nm of niobium are etched, the Cu using the Ion Beam etcher, with a working presure of 3-4$\times 10^{-4}$ mbar and the Nb using Plasma etching, using CF_4 and O_2 gasses.

Finally, the resistance which is left on top of the structure is washed away using the remover.

In this way, a planar Josephson junction with a normal metal as a weak link is obtained.

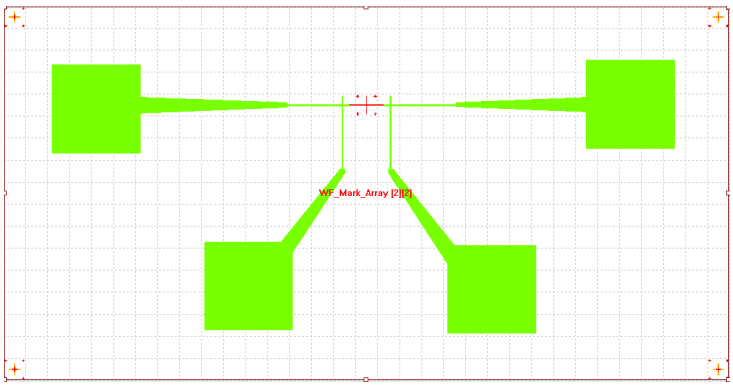

Fig. 3.1.1. Pattern of the structure in the electron beam. The top contacts are used to apply a current and the bottom contacts to measure the voltage that is generated across the juction.

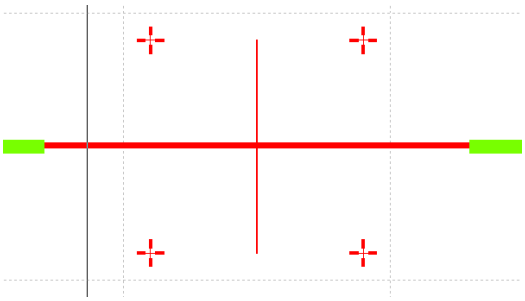

Fig. 3.1.2. Draft of the Josephson junction used in the electron beam. The vertical red line in the figure represents where the gap of the junction is. This gap is made in the second step of the e-beam using positive resist. We will work with lengths between 75 nm and 300 nm.

Figure 3.1.3. shows a real image of a Josephson junction taken with the Scanning Electron Microscope.

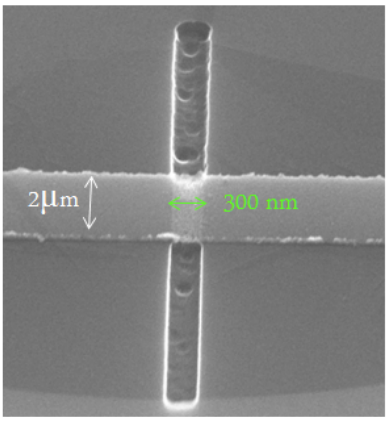

Fig. 3.1.3. Image taken with the Scanning Electron Microscope of a Josephson junction. Niobium electrodes are connected through a 300 nm copper weak link.

In this thesis 3 S-N-S junctions are analyzed, 2 with a length of 150 nm and one with 300 nm. They are named as JJ.N1.150, JJ.N2.150 and JJ.N.300. 3 S-N/F-S junctions are also analyzed, with lengths of 75 nm, 150 nm and 200 nm. The names given for these junctions are: JJ.NF.75, JJ.NF.150 AND JJ.NF.200.

3.2 Measurements

The Josephson junctions are measured in the '7 Tesla' cryostat, cooling them down to temperatures below their critical temperature. With this type of standard cryostat temperatures between 300 K and 2 K can be measured.

The sample is mounted in the insert and it is placed in a rotating sample holder. This allows the user to fix the angle with respect to the applied magnetic field.

In order to measure the devices, four terminal measurements are used. In the top contacts of the structures (see Fig. 3.1.1) it is applied a current and with the bottom contacts the voltage of the junction is measured. The current is injected using a DC voltage and different resistances. The voltage generated across the junction is measured with a nanovoltmeter, which has a noise level between 100-200 nanovolts.

Chapter 4

Results

In this chapter the most relevant results are shown.

In the first part(4.1), Nb-Cu-Nb Josephson junctions are analyzed in order to have a clear understanding of the Josephson effect and the proximity effect in superconductor-normal interfaces. The niobium and the copper layers are 50 nm thick. The critical current of the Josephson junctions is analyzed, plotting V vs. I curves. The temperature dependence of critical current is studied, and the different behaviors of the junction of 150 nm and the one of 300 nm.

Having analyzed S-N-S junctions and having them as a reference, we are able to move on to S-N/F-S junctions and investigate the influence of the ferromagnet on the proximity effect.

Therefore, in the second part of this Chapter(4.2), Nb-Cu/Co-Nb junctions are studied and it is examined how 10 nm of Cobalt next to the normal metal affects the junction's properties . The different gap lengths used are: 75 nm, 150 nm and 200 nm.

4.1 Nb-Cu-Nb junctions

S-N-S Josephson junctions with gap lengths of 150 nm and 300 nm are analyzed, 2 of 150 nm and 1 of 300 nm. The critical temperatures of the structures have values between 4.5-5 K.

The junction JJ.N1.150 is first characterized.

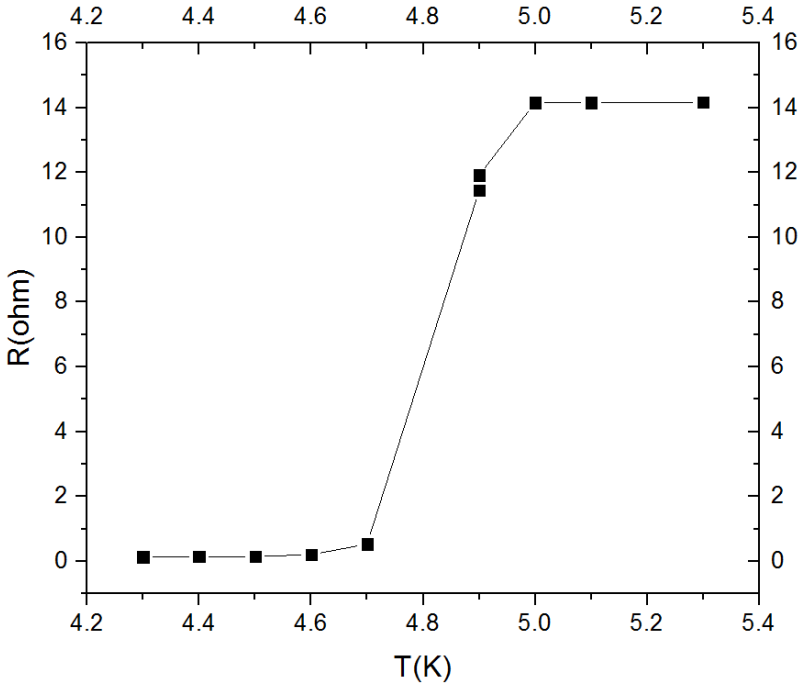

Fig. 4.1.1 Resistance(R) of the junction JJ.N1.150 is plotted as a function of the temperature(T). A superconducting transition can be seen at temperatures around 4.8 K.

The critical temperature of the structure JJ.N1.150 is $T_c = 4.8$ K. A temperature of 4 K is fixed and voltage versus current plots are made in order to determine the critical current.

Two V vs. I curves of the same structure are shown. In the first V-I curve, figure 4.1.2, currents from -2 mA to 2 mA are applied. A zoom in is performed for a small range in the current, from -600 μA to +600 μA, figure 4.1.3.

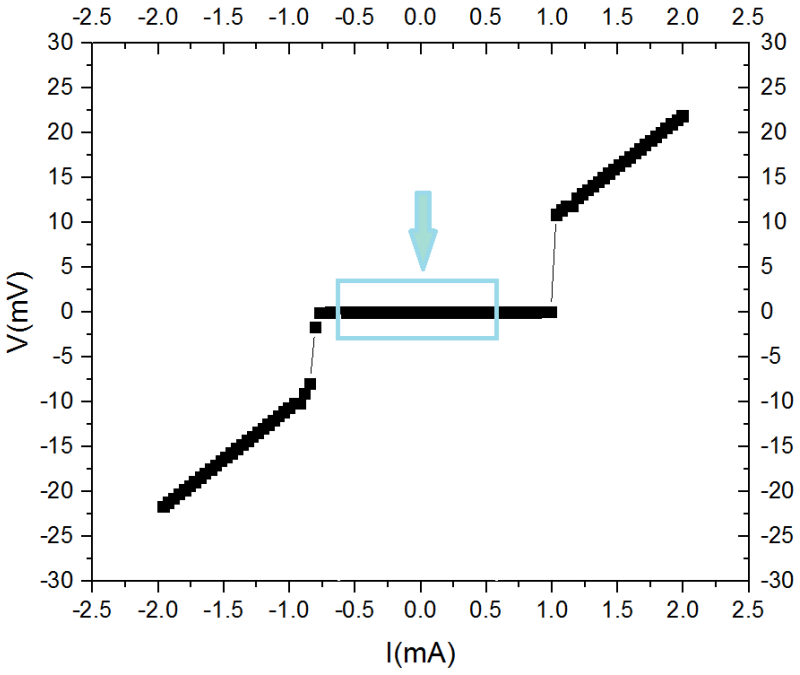

Fig. 4.1.2 Voltage(V) versus current(I) of JJ.N1.150, from $I_{min} = -2$ mA to $I_{max} = 2$ mA. A sharp superconducting transition can be found at around the value 895 μA. The blue square shows the range of the currents which is analyzed in the next plot. This V-I curve is taken at fixed temperature of 4 K and the critical temperature of the structure is $T_c = 4.8$ K.

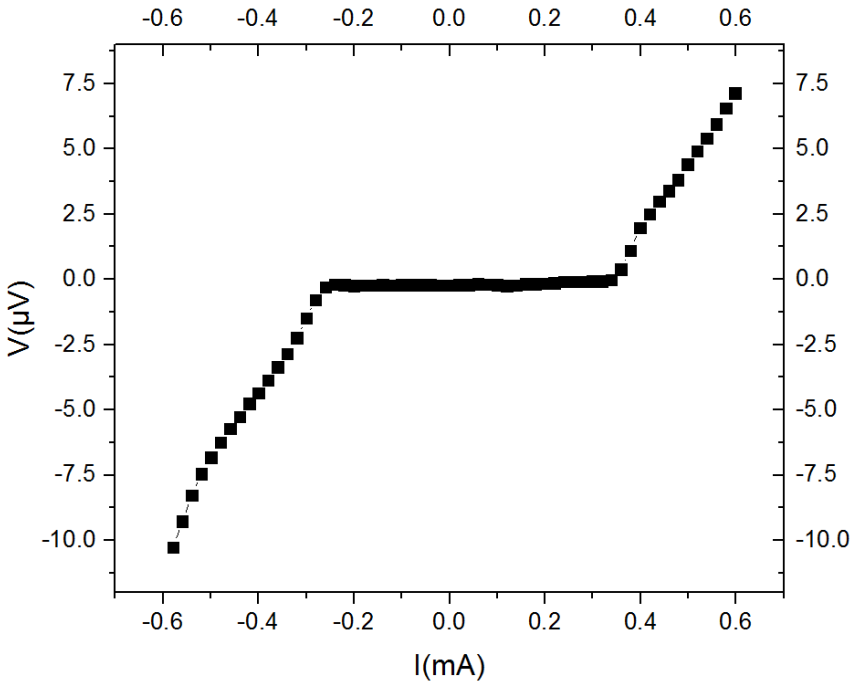

Fig. 4.1.3 Voltage(V) versus current(I) of JJ.N1.150, from $I_{min} = -600$ μA to $I_{max} = 600$ μA. Another superconducting transition can be found, but in this case less sharp and at a much smaller value of the current, 300 μA. This V-I curve is taken at fixed temperature of 4 K and the critical temperature of the structure is $T_c = 4.8$ K.

There are two superconducting transitions: the first one occurs when the niobium becomes superconductor, at $I_{c,Nb}$=895 μA; and the second transitions occurs when the normal metal of the junction gets proximized, meaning that a supercurrent can flow through the weak link. This second transitions occurs at $I_{c,jj} = 300$ μA. It should be noted that the critical current is defined as the value in which the voltage reaches 100-200 nanovolts (noise level) and the resistance starts to oscillate.

An asymmetry in the V-I curve can be observed. This effect has been observed not only in this structure, but also in others. We believe that this behavior could be due to two possible reasons: it could be caused by the measurement setup, by an offset in the electronics; or because the junctions themselves are not completely homogeneous. As a consequence of this asym-

metric behavior, the critical current is defined as the average of the value in the negative side and the value of the positive.

The resistance is defined as simply the ratio of the measured voltage and current, $\frac{V}{I}$ (Fig. 4.1.4). The weak link of this junction shows a normal resistance around the value of 20 mΩ. It can be seen in Fig. 4.1.5, how the normal metal gets proximized and once the current goes below the critical current of the junction, the structure becomes completely superconductor: $R = 0$. It should be noted that an exact zero value is never obtained, this is because there is always noise. This noise is generally between the values 100 and 200 nanovolts, which gives a minimum resistance of the order of 10^{-3} Ω. A clear indication that the measured resistance is due to the noise is its oscillating behavior around the absolute zero.

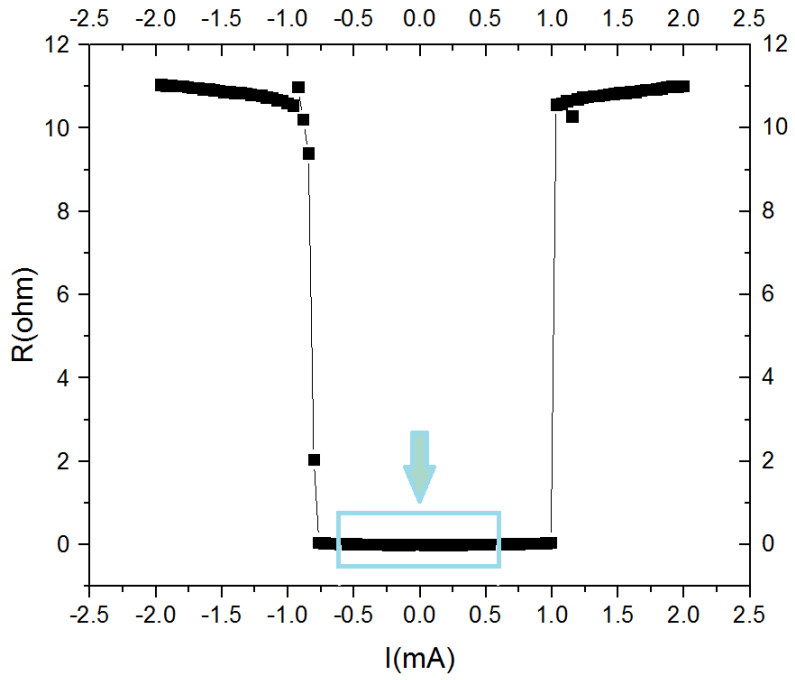

Fig. 4.1.4 Resistance(R) versus current(I) for the junction JJ.N1.150, from $I_{min} = -2$ mA to $I_{max} = 2$ mA. A sharp superconducting transition is shown, the values of the resistance drop from roughly 11 Ω to values close to zero. The blue square shows the range of the currents which is analyzed in

the next plot. This R-I curve is taken at fixed temperature of 4 K and the critical temperature of the structure is $T_c = 4.8$ K.

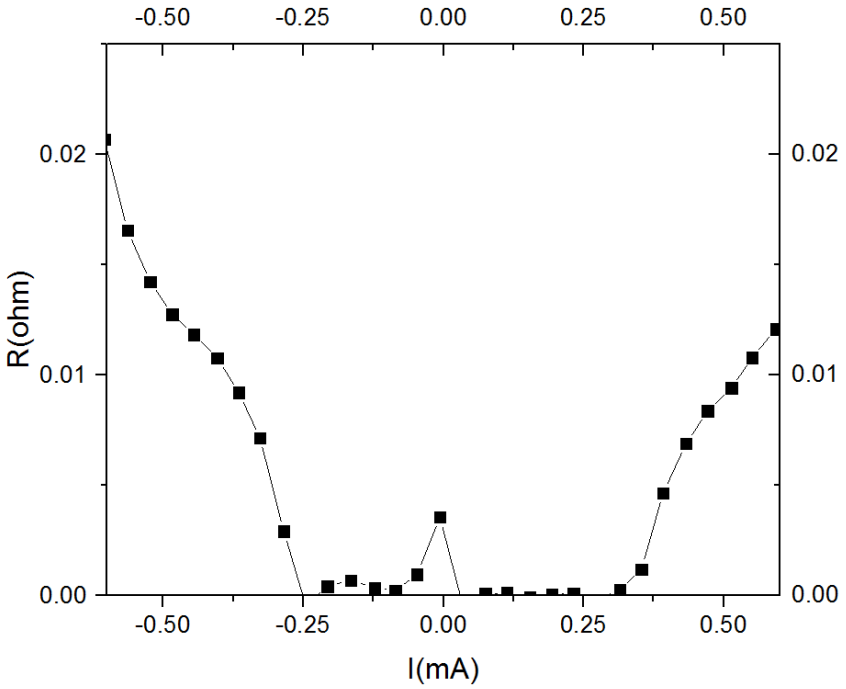

Fig. 4.1.5 Resistance(R) versus current(I) for the junction JJ.N1.150, from $I_{min} = -600\ \mu A$ to $I_{max} = 600\ \mu A$. In this figure is shown the second transition. After this, the normal metal of the weak link behaves as a superconductor showing $R = 0$. This V-I curve is taken at fixed temperature of 4 K and the critical temperature of the structure is $T_c = 4.8$ K.

Now, it is explored the different behavior of the junctions JJ.N2.150 and JJ.N.300, the first one has 150 nm gap length and the second one, 300 nm.

The critical temperature of these two junctions is around 4.5 K, this is slightly smaller than the junction studied above.

It is shown the voltage as a function of the current of JJ.N2.150 at 2.6 K, for a small range (-1 mA, 1 mA) and a longer range (2 mA, -2 mA) of the current.

In many cases, an hysteric behavior in the transition of the superconductor is observed, in the long range of the current (Fig. 4.1.7). This has not been observed in the transition of the normal metal. We believe that the origin of this hysterisis phenomenom is thermal. The reason may be that when the electrons go through the transition from the the superconducting state to the normal metallic state, they gain an additional thermal energy. As a consequence, the superconducting state is recovered at a smaller value of the current [13].

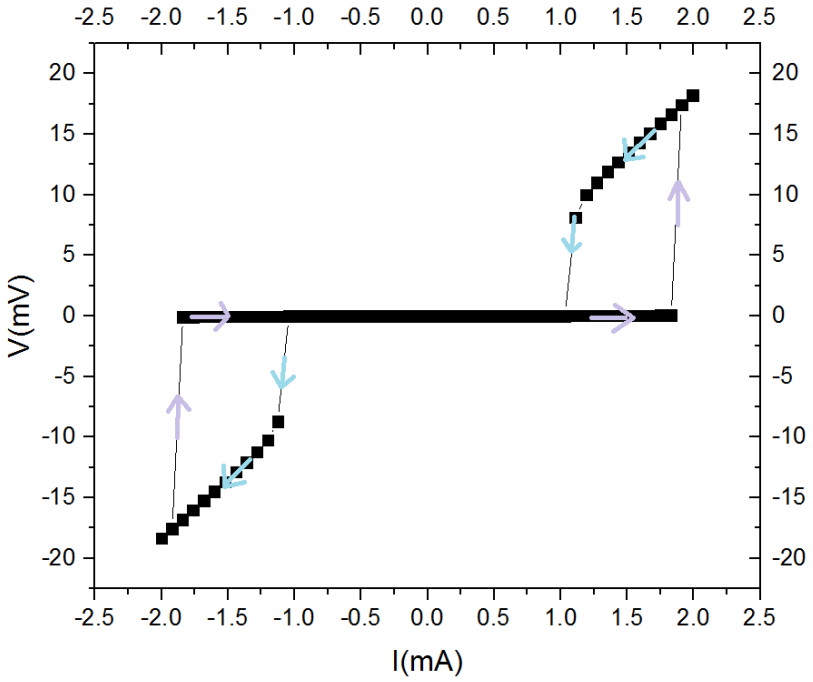

Fig. 4.1.6. Hysteresis in the voltage(V) versus current(I) curve of JJ.N2.150, from - 2mA to 2 mA. This V-I curve is taken at fixed temperature of 2.6 K and the critical temperature of the structure is $T_c = 4.5$ K

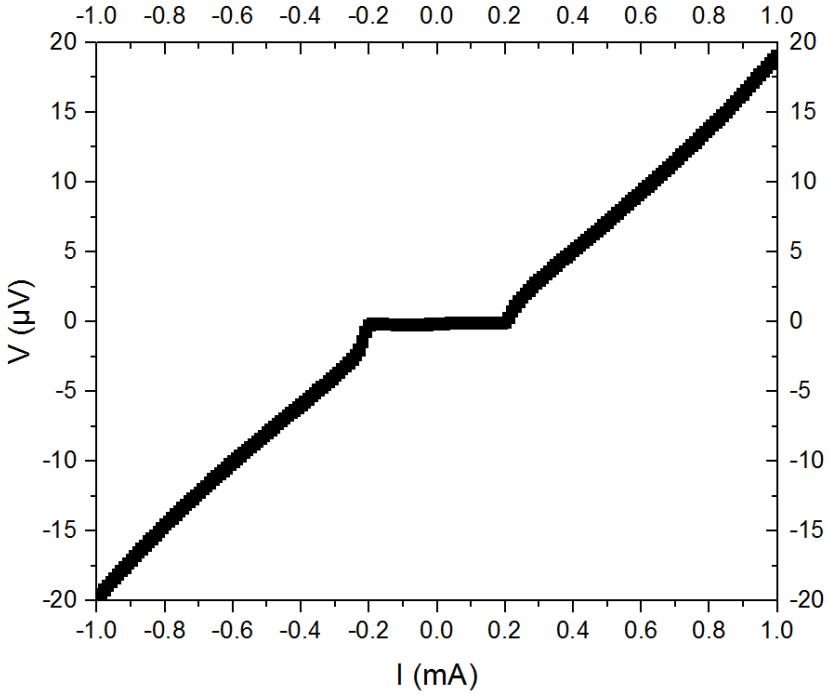

Fig. 4.1.7. Voltage(V) versus current(I) curve of JJ.N2.150, from - 1mA to 1 mA. It can be seen the superconducting transition of the normal metal of the junction. This V-I curve is taken at fixed temperature of 2.6 K and the critical temperature of the structure is $T_c = 4.5$ K

The critical current of the josephson junction at T= 2.6 K is I_c(150 nm)= 190 μA.

The measured normal resistance of the junction at 2.6 K is R_N(150 nm)= 22.4 $m\Omega$.

With a longer gap length it should be expected a smaller critical current, because the proximity effect is weaker as longer is the junction. And this is exactly what it is observed in the V-I curve of the junction JJ.N.300 (Fig. 4.1.8) which has double the gap length of the one studied above.

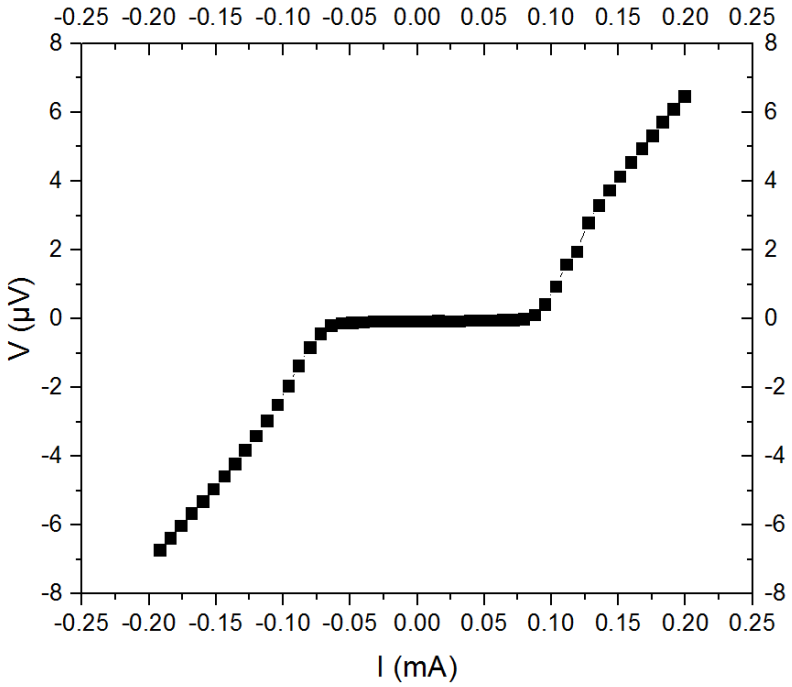

Fig. 4.1.8. Voltage(V) versus current(I) curve of JJ.N.300, from -0.25 mA to 0.25 mA. In this case, the superconducting transition of the normal metal occurs at smaller values of the critical current than the ones of the JJ.N2.150(Fig. 4.1.7). This V-I curve is taken at fixed temperature of 2.6 K and the critical temperature of the structure is $T_c = 4.5K$

At 2.6 K, the critical current of the Josephson junction is I_c(300 nm)= 64 μA.

The measured normal resistance of the junction at 2.6 K is R_N(300nm)= 56 $m\Omega$.

In the following pages it is shown the dependence on the temperature of the critical current, for the junction with 150 nm and the one with 300 nm. This analysis allows having a better insight into the properties of the S-N-S junctions, as parameters such as the Thouless energy can be obtained. This is considered to be the characteristic energy of the phenomenons arising in SN interfaces[14]. This analysis could provide with an understanding of the transparency in the interface and homogeneity of our junctions.

In the following plot,(Fig. 4.1.8), V-I curves of the JJ.N.300 junction at some different temperatures are shown, and it is noticeable how the increase in the temperature implies a decrease in the critical current of the jnction.

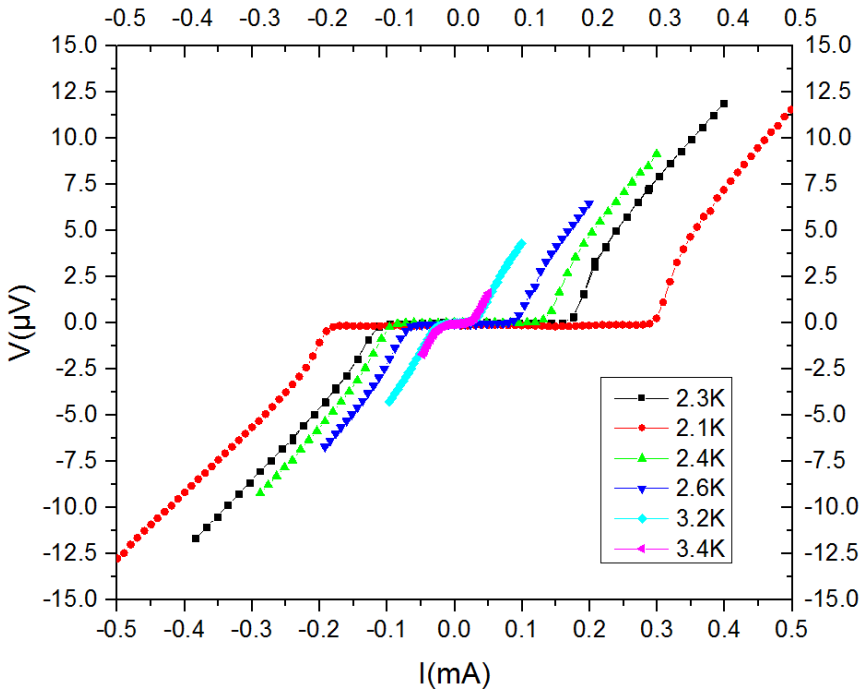

Fig. 4.1.9. Voltage(V) versus current(I) curves of the junction JJ.N.300 at different temperatures. At higher temperatures the value of the current in which the voltage becomes zero is smaller, meaning that the superconductivity is weaker as closer is the temperature to its critical value. The critical temperature is 4.5 K.

In the following plots it is shown I_c vs. T curves of the two different junctions.

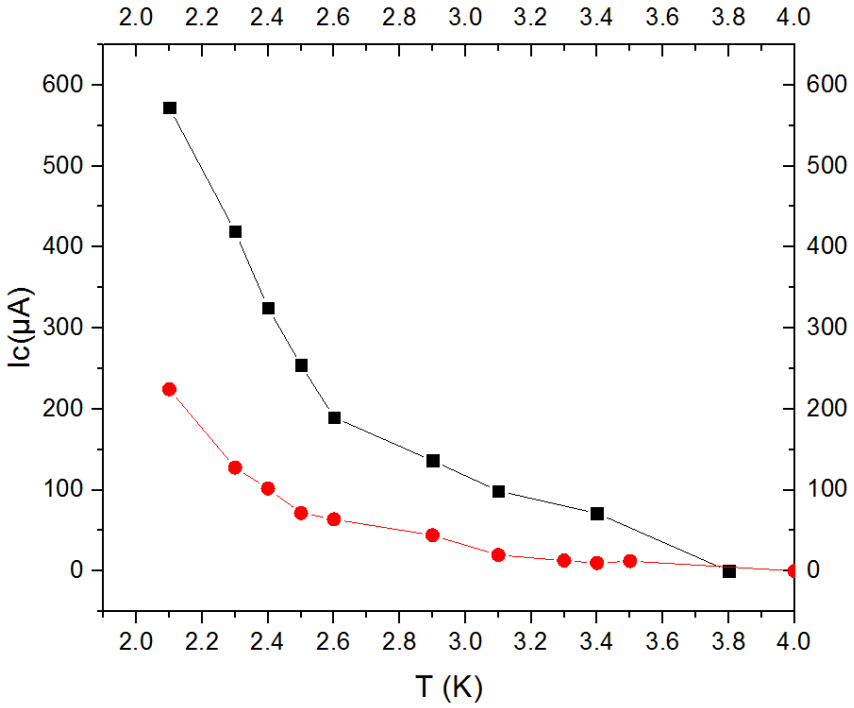

Fig. 4.1.10. Critical current(I_c) as a function of temperature(T) of the junction JJ.N2.150(black, squares) and JJ.N.300(red, circles).

4.2 Nb-Cu/Co-Nb junctions

As a next step, S-N/F-S junctions are analyzed. Their lengths are 75 nm for the JJ.NF.75, 150 nm for the JJ.NF.150 and 200 nm for the JJ.NF.200. We analyze V vs. I curves at temperatures of 2.4 K and 3.1 K. The critical temperature of this junctions is around 4.5 K.

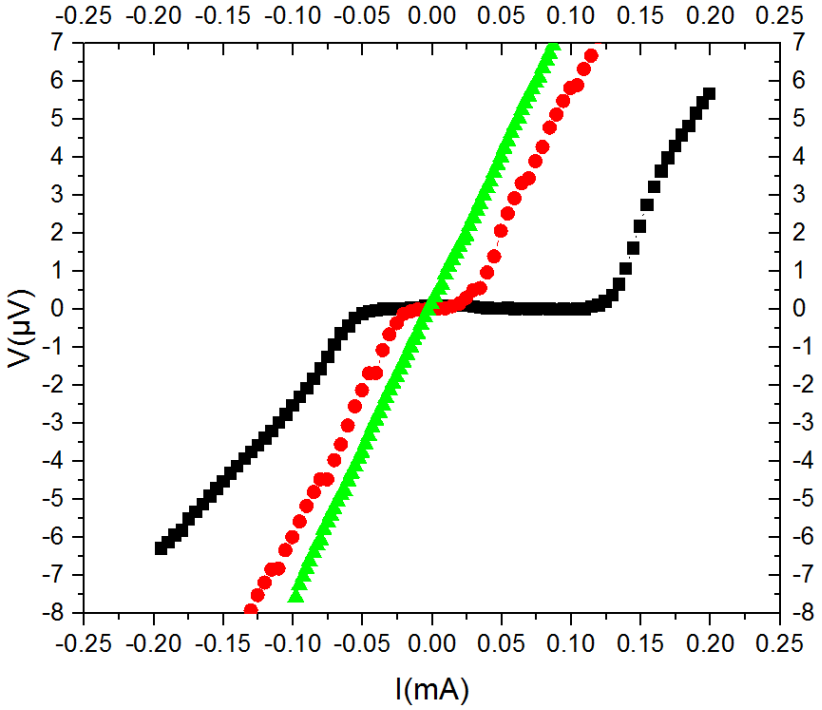

Fig. 4.2.1. Voltage(V) versus current(I) for the junctions JJ.NF.75(black, squares), JJ.NF.150(red, circles) and JJ.NF.200(green, triangles) at 2.4 K and a T_c of 4.5 K. In this figure the behavior of three junctions with different gap length is plotted, and each one shows a different critical current. The junction JJ.NF.75 shows the highest I_c. The junction JJ.NF.150 shows resistance zero at a smaller critical current. However, the junction JJ.NF.200 does not show any Josephson effect, and gives a finite normal resistance.

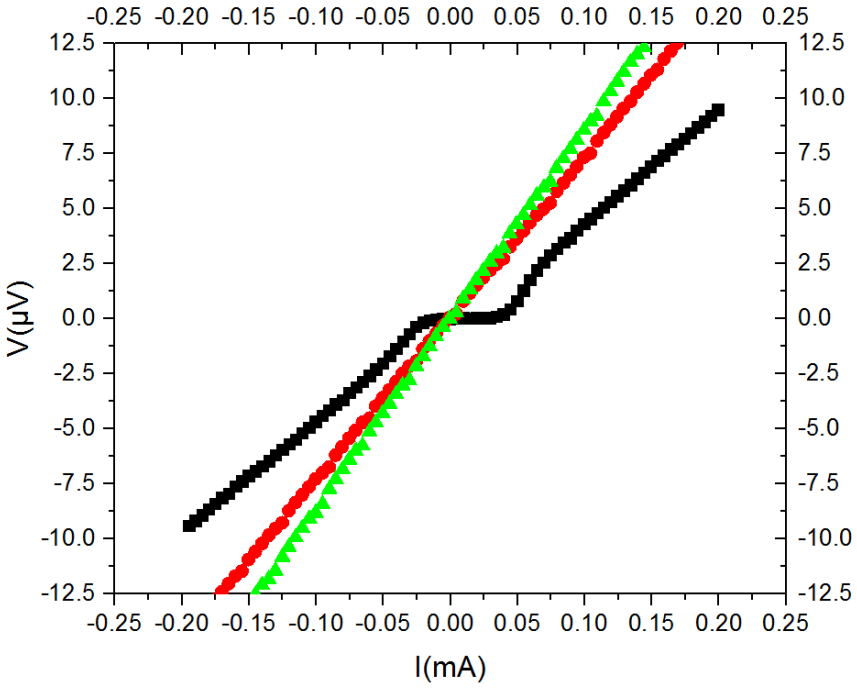

Fig. 4.2.2. Voltage(V) versus current(I) for the junctions JJ.NF.75(black, squares), JJ.NF.150(red, circles) and JJ.NF.200(green, triangles) at 3.1 K and a T_c of 4.5 K. At a temperature of 3.1 K, the JJ.NF.75 shows the superconducting transition of the weak link at a certain current, while the JJ.NF.150 and JJ.NF.200 present the typical Ohmic behaviur of the normal metals. It can be seen that the slope of the JJ.NF.200 is bigger than the one of JJ.NF.150, meaning that junction with a gap length of 200 nm has a higher normal resistance than the one with a gap length of 150 nm: the longer is the length, the higher the resistance(equation 5.1).

In the following table we summarize the critical currents and the normal resistances for S-N/F-S junctions at these two different temperatures.

Junction	T(K)	$R_N(m\Omega)$	$I_c(\mu A)$
JJ.NF.75	2.4	43	73.3
JJ.NF.75	3.1	54.2	21
JJ.NF.150	2.4	76.5	13.35
JJ.NF.150	3.1	73.3	0 (no supercurrent)
JJ.NF.200	2.4	77.6	0 (no supercurrent)
JJ.NF.200	3.1	86	0 (no supercurrent)

Fig. 4.2.3. Critical current(I_c) and normal resistance(R_N) for structures JJ.NF.75, JJ.NF.150 and JJ.NF.200 at 2.4 K and 3.1 K. The T_c of the structure is 4.5 K.

In figure 4.2.4 it is plotted the values of the critical currents for the different gap lengths at 2.4 K and 3.1 K.

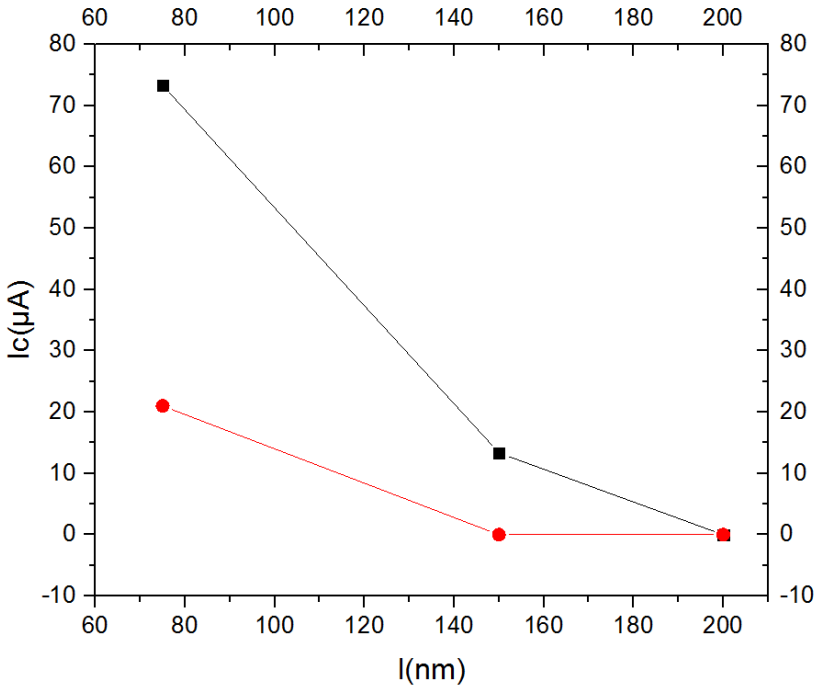

Fig. 4.2.4. Critical current(I_c) versus length(l) of S-N/F-S junctions at 2.4 K(black, squares) and 3.1 K(red, circles). The T_c of the structure is 4.5 K. Longer gaps have smaller critical currents. It could be noted that, at both

temperatures, the junction with a gap length of 200 nm does not show the Josephson effect.

It should be noted that a deeper analysis of the temperature dependence of I_c in S-N/F-S junctions has not been performed due to time constraints.

However, comparing the measured critical currents for S-N-S and S-N/F-S junctions at temperatures 2.4 K and 3.1 K (Fig. 4.2.5) allows us to clearly notice the effect of the ferromagnet on the critical currents.

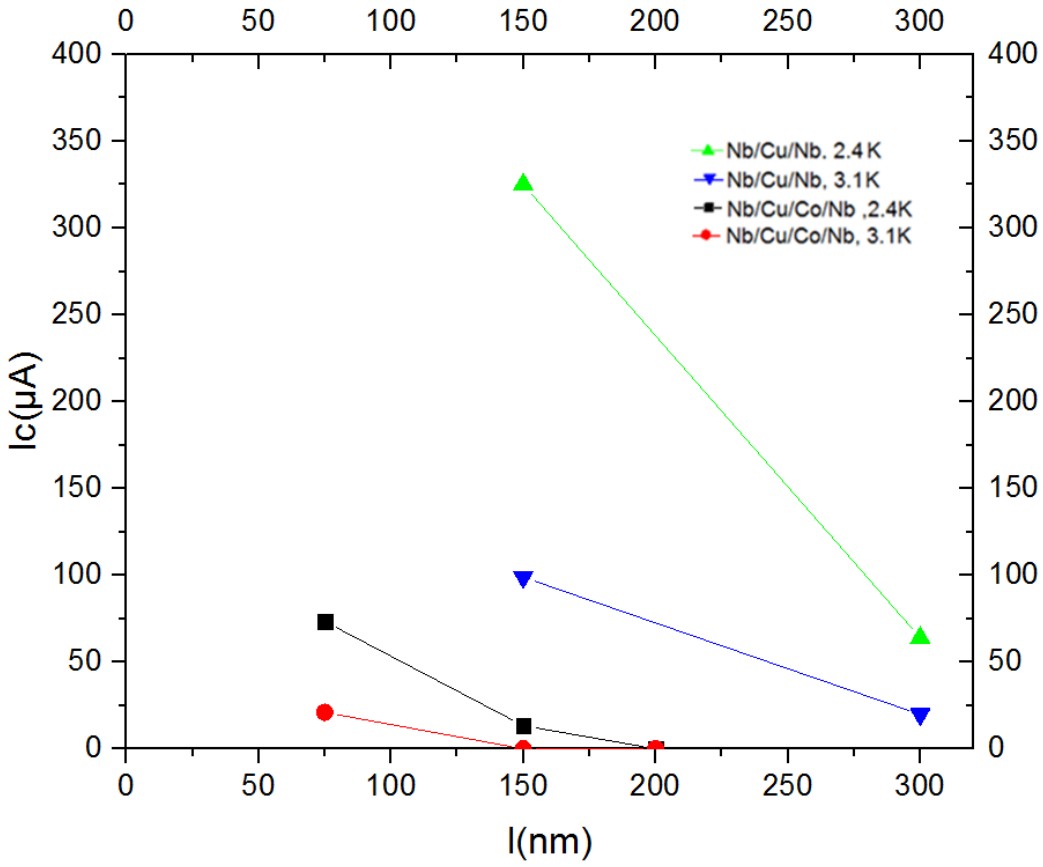

Fig. 4.2.5. Critical current(I_c) as a function of the length of the gap(l) of S-N-S and S-N/F-S junctions at 2.4 K and 3.1 K. The crititical temperatures for both type of the junctions, Nb-Cu-Nb and Nb-Cu/Co-Nb, are roughly around 4.5 K. Junctions of the type Nb-Cu-Nb: at $T = 2.4$ K are represented

by a green curve with triangles pointing up, and at $T = 3.1$ K by a blue curve with triangles pointing down. Junctions of the type Nb-Cu/Co-Nb: at $T = 2.4$ K are represented by a black curve with squares, and at $T = 3.1$ K by a red curve with circles. A dramatic supression of the critical currents of the Nb-Cu/Co-Nb junctions compared with the ones of Nb-Cu-Nb junctions is clearly noticeable. This figure shows how 10 nm of Co have a strong influence on the Proximity effect when placed next to the 50 nm of Cu.

Chapter 5

Discussion

In this chapter, the results presented in chapter 4 are explained and discussed. The behavior of S-N-S junctions and S-N/F-S junctions is analyzed. The goal of the study of S-N-S junctions(5.1), is to have a clear understanding of the proximity effect in the measured structures. Having this as a reference, the next step is to study S-N/F-S junctions(5.2) and discuss the effect of placing a ferromagnet next to the normal metal, which is the ambition of this thesis.

5.1 S-N-S junctions

Firstly, the junction JJ.N1.150 is characterized, which is a Superconductor-Normal metal-Superconductor junction with a gap length of 150 nm. The T_c of the structure is 4.8 K (Fig. 4.1.1) and the measurements are performed at a fixed temperature of 4 K. There are two different critical currents: the first one is the critical current of the superconductor itself, $I_{c,Nb} = 895\ \mu A$ (Fig. 4.1.2), and the second one is smaller, and it is the critical current of the normal metal of the junction, $I_{c,jj} = 300\ \mu A$ (Fig 4.1.3). Hence, at a certain current the niobium leads become superconductor but the gap has still a resistance of the order of $10^{-2}\ \Omega$. This cannot be appreciated in Fig. 4.1.4, but when zooming into a smaller range of currents(Fig. 4.1.5), a second transition can be seen and also, the value of the current at which the resistance becomes completely zero. The resistance of the normal metal is measured experimentally. For a gap length of 150 nm and a temperature of 4 K, it has a value around $R_N = 28\ m\Omega$.

The expected normal resistance of the weak link is:

$$R_N = \rho_{Cu}\frac{l}{wd_N} \tag{5.1}$$

where ρ_{Cu} is the resistivity of the copper, w is the width, l is the length and d_N is the thickness of the gap.

The resistivity of the copper is estimated by measuring the resistance of a copper bar of 0.21 mm length, 10 μm width and 50 nm of thickness, which showed a resistance of 6.7 Ω and hence, a resistivity of $\rho_{Cu} = 1.58 \times 10^{-8}$ Ωm. It was measured at temperatures around 4 K. This resistivity gives us a value of the normal resistance of 23 $m\Omega$.

The expected value and the experimental value of the normal resistance are in good agreement. It should be noted that the gap does not show the ideal behavior. Theoretically, the gap should present a finite resistance between the $I_{c,Nb}$ and the $I_{c,jj}$ and then, the normal metal of the weak link should experience a sharp superconducting transition and R should reach zero. Instead, the weak link gets proximized slowly, decreasing the normal resistance until it completely vanishes(Fig. 4.1.5). This means that at a certain current, which is the critical current of the Josephson junction, the Cooper pairs from one superconducting electrode are induced into the other one due to the phenomenon of Andreev reflection(Fig. 2.3.3).

The next step is to analyze the behavior of the junctions JJ.N2.150 and JJ.N.300 at different temperatures and to compare them with the expected values. In order to perform this analysis, some theoretical study of the S-N-S junctions adapted from reference [15] is shown first.

To begin with, it must be mentioned one of the most important parameters in order to analyze the S-N-S junctions: the Thouless energy, ϵ_c. This parameter is considered to be the natural energy of the proximity effect and it is given by:

$$\epsilon_c = \frac{\hbar D}{L^2} \tag{5.2}$$

where L is the length of the junction and D is the diffusion coefficient.

This last one is given by:

$$D = \frac{v_F^2 \tau}{3} \tag{5.3}$$

where v_F is the Fermi velocity and τ is the relaxation time.

Using the Drude model we obtain the relation $\tau = \frac{m}{\rho n e^2}$. Hence the expression for the diffusion coefficient takes the form of:

$$D = \frac{v_F^2 m}{3ne^2\rho} \tag{5.4}$$

where n is the electron density, $n = 8.53 \times 10^{28}\ m^{-3}$; v_F is the Fermi velocity, $v_F = 1.58 \times 10^6\ m/s$; e is the electron charge, $e = 1.6 \times 10^{-19}$ C; m is the electron mass, $m = 9.1 \times 10^{-31}$ kg and ρ is the resistivity, which we measured to be $\rho_{Cu} = 1.58 \times 10^{-8}\ \Omega$ m. The value of the diffusion coefficient is then $D = 220\ cm^2/s$.

It can be studied the dependence of the value $I_c R_N e/\Delta$ at $T = 0$ K as a function of the ratio ϵ_c/Δ. Δ is the energy gap, which has a value of $1.76 k_B T$. This dependence can be seen in the following figure (5.1.1), and the two different regimes of the S-N-S junctions can be apreciated: short junction regime ($\Delta < \epsilon_c$) and long junction regime($\Delta > \epsilon_c$).

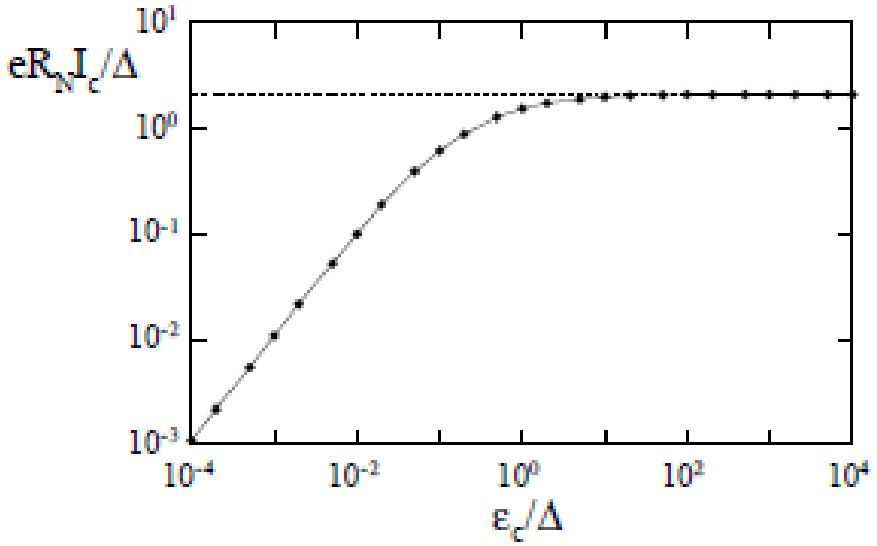

Fig. 5.1.1 Calculated dependence of the zero temperature $eR_N I_c$ product in units of Δ as a function of the ratio ϵ_c/Δ. I_c is the Josephson critical current, R_N the normal state resistance, ϵ_c is the Thouless energy and Δ is

the superconducting gap of S. The long junction regime is on the left part of the graph where $\epsilon_c < \Delta$, the short junction regime is on the right part where $\epsilon_c > \Delta$. This figure is taken from reference [15].

The temperature dependence of the value $I_c R_N e$, for junctions belonging to the long junction regime is plotted in figure 5.1.2:

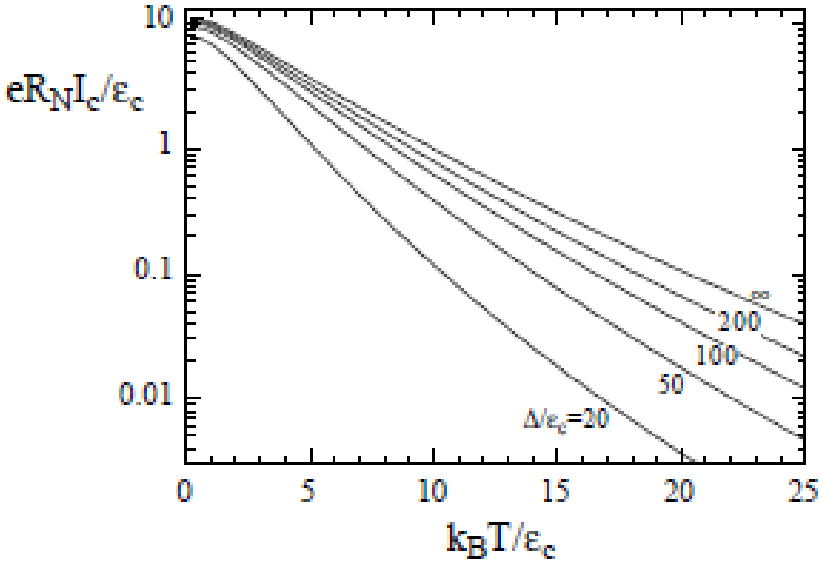

Fig. 5.1.2 Calculated temperature dependence of the $I_c R_N e$ product. The different curves correspond to various values of the ratio Δ/ϵ_c in the long junction regime. The curve for $\Delta/\epsilon_c \to \infty$ is universal in the sense it does not depend on Δ. This figure is taken from the reference[15].

When $\Delta/\epsilon_c \to \infty$ the temperature dependence of the critical current is given by[15]:

$$eR_N I_c = \frac{32}{3+2\sqrt{2}} \epsilon_c [\frac{L}{L_T}]^3 \exp(-L/L_T) \tag{5.5}$$

where L is the length of the junction and $L_T = \sqrt{\hbar D/2\pi k_B T}$ is the characteristic thermal length in the diffusive limit.

In this long limit regime, Josephson junctions with a perfect transparency show the relation:

$$\frac{I_c(T=0)R_N e}{\epsilon_c} = 10.82 \tag{5.6}$$

After this brief theoretical analysis, the measured junctions JJ.N2.150 and JJ.N.300 are discussed.

At a temperature of 2.6 K, the critical current of the junction with 150 nm is $I_c = 190\ \mu A$ (Fig. 4.1.7). and the one with 300 nm is $I_c = 64\ \mu$A (Fig. 4.1.8).

The I_c of the short junction is higher than the I_c of the larger one. This statement is consistent with the theory, as with longer gaps the superconductivity of the normal metal is weaker, meaning a smaller critical current. This is due to the fact that the order parameter which characterizes the superconducting state, decreases as the length of the junction becomes longer(Fig. 2.1.4): the proximity effect becomes weaker for longer lengths.

Considering the equation in 5.1 we expect to have the following normal resistances: for the junction with 150 nm length $R_N = 23\ m\Omega$ and the one with 300 nm, $R_N = 66\ m\Omega$, which are in good agreement with the values obtained experimentally: at 2.6 K, for a length of 150 nm it is measured 22.4 mΩ, and for a length of 300 nm, 56 mΩ.

In the following paragraphs the temperature dependence of these two planar junctions is examined, as it is one important feature of the S-N-S junctions.

The critical current is dependent on the temperature as an increase in T implies thermal excitations in the metal, causing the faster breaking of the Cooper pairs. Therefore, the closer the T is to the T_c, the smaller is the Ic.

In Fig. 4.1.9 it is analyzed the V-I curves for different temperatures, and it is shown that the increase in the temperature decreases the critical current, meaning a weaker superconductivity in the junction. The temperature dependence of I_c can be clearly seen in Fig. 4.1.10, where it is plotted the critical current as a function of temperature for 2 different junctions, one with a length of 150 nm and the other of 300 nm. It can be seen how, once the temperature is close enough to the critical value, the junction looses its superconducting properties. The temperature has a strong effect on the crit-

ical current. It can also be appreciated how the length of the gap affects the critical current. For the junction of 150 nm, the critical currents are higher than for the junction of 300 nm, as it has been discussed earlier in this chapter.

Taking into account the expression of the Thouless energy given in equation 5.2, the junctions with a gap length of 150 nm have a theoretical value of 644.1 μeV , and for those junctions with 300 nm length the value is 161 μeV.

In order to obtain the experimental value of the Thouless energy from our measurements, we use the temperature dependence of the critical current given by the equation 5.5:

$$eR_N I_c = \tfrac{32}{3+2\sqrt{2}}\epsilon_c[\tfrac{L}{L_T}]^3 \exp(-L/L_T)$$
$$ln(eR_N I_c) = ln(\tfrac{32}{3+2\sqrt{2}}\epsilon_c[\tfrac{L}{L_T}]^3 \exp(-L/L_T))$$
$$ln(I_c) = ln([\tfrac{L}{L_T}]^3) - (-L/L_T) + ln(\tfrac{32}{3+2\sqrt{2}}\epsilon_c)$$

The last term is just a constant.

Taking into account the expressions for L_T and ϵ_c, we finally arrive at the following equation:

$$[ln(I_c) - \frac{3}{2}ln(T)] = \sqrt{\frac{2\pi k_B}{\epsilon_c}}\sqrt{T} + const. \tag{5.7}$$

By using the values of the critical currents at different tenperatures, it is plotted $[ln(I_c) - \frac{3}{2}ln(T)]$ versus $\sqrt{T}$ (see figure 5.1.3 below) and the following values for the slopes are obtained:

$l = 150nm$, $\sqrt{\frac{2\pi k_B}{\epsilon_c}} = -7.23$, which gives a Thouless energy of $\epsilon_c = 10.4$ μeV.

$l = 300nm$, $\sqrt{\frac{2\pi k_B}{\epsilon_c}} = -8.96$, which gives a Thouless energy of $\epsilon_c = 6.72$ μeV.

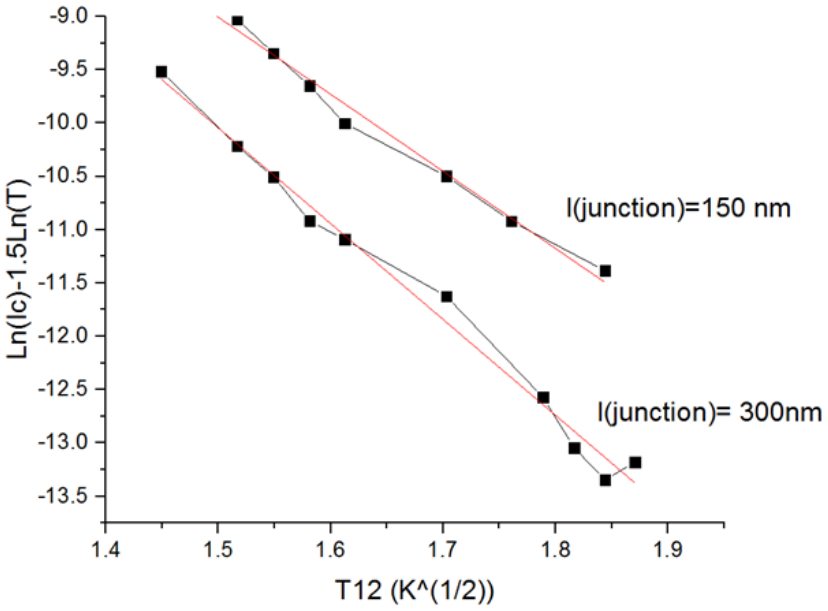

Fig. 5.1.3. In this graph it is shown the value of $[ln(I_c) - \frac{3}{2}ln(T)]$ as a function of $\sqrt{T}$. For the both junctions: JJ.N2.150 and JJ.N.300. In this way, the slope, which has a value of $\sqrt{\frac{2\pi k_B}{\epsilon_c}}$ can be derived, and hence, a experimental value for the Thouless energy can be obtained. It can be seen that the two junctions behave very similar.

It can be clearly seen a big difference between the experimental values of the Thouless energy and the theoretical values. We believe that the main reason of this difference is that our junctions do not fulfill the condition $\Delta \gg \epsilon_c$ that equation 5.5 requires. The ratio between the energy gap and the theoretical Thouless energy for the junction with 150 nm length is 1.1, and for the one with 300nm length is 4.3. Even if they are in the long regime where $\Delta > \epsilon_c$, the values are really small. It can be seen in Fig. 5.1.1 that when ϵ_c and Δ have similar values, which is our case, we get values which are very close to the short regime. Since 5.5 equation only holds in the long limit

regime, $\Delta/\epsilon_c \to \infty$, we should use the general expression for the temperature dependence of the critical current[15]:

$$eR_N I_c = 64\pi K_B T \sum_{n=0}^{\infty} \frac{L}{L_{\omega_n}} \Delta^2 \exp\left(-L/L_{\omega_n}\right)/[\omega_n + \Omega_n + \sqrt{2(\Omega^2 + \omega_n \Omega_n)^2}] \tag{5.8}$$

In this expression $\omega_n = (2n+1)\pi k_B T$ is the Matsubara frequency, $\Omega_n = \sqrt{\omega_n^2 + \Delta^2}$ and $L_{\omega_n} = \sqrt{\frac{\hbar D}{2\omega_n}}$.

We expect that using the expression 5.8 to obtain the experimental Thouless energies of the measured S-N-S junctions would provide us with values more consistent with the theoretical ones. However, due to time constraints, this analysis has not been performed.

It could also be pointed out that the estimations of the ϵ_c found in literature[15] take into account the full range of temperatures, and in particular the ones really close to zero; while in our study, it is used a much more limited range.

Our values could also be slightly affected by an overestimation of the expected ϵ_c, the lengths of the junctions could be slightly bigger than the ones we are considering for the calculations, and also, the expression of the diffusion coefficient is given by the Drude model in which we use standard values for the Fermi velocity or the density of electrons that can differ from the real ones.

As a consequence of the fact that the measured Josephson junctions are close to the short regime, we expect to have a ratio between the value $I_c R_N e$ and the Thouless energy much smaller than 10.82, which is the one obtained theoretically in the long limit regime. At 2.1 K, which is the smallest temperature that can be reached, and using the calculated theoretical values of the Thouless energy, the ratios obtained are very small: 0.02 for the junction with 150 nm and 0.1 for the one with 300 nm.

Although we believe that the main reason for this is that the junctions are far away from the long limit regime, other physical aspects that could also affect are, for example, that our gaps are not fully homogeneous, meaning that the supercurrent does not flow through all the volume of the weak link in the same way, or that there is not a perfect transparency in the SN interface.

Nonetheless, our junctions are quite well reproducible, which encourages us to think that our planar Josephson junctions are reliable to work with.

5.2 S-N/F-S junctions

Until now, Nb-Cu-Nb junctions have been characterized studying the temperature and the length dependence of the Josephson critical current. The obtained results have been analyzed and compared with the expected values. In this section, S-N/F-S junctions are investigated, to study the effect of the ferromagnet on the critical current of the junction.

We analyzed 3 different junctions, with a different length, at 2 different temperatures: 2.4 K and 3.1 K.

For the junction with a length of 200 nm at either 2.4 K and 3.1 K, the superconductivity is completely destroyed meaning that the resistance of the normal metal does not become zero at any value of the current(green curve in Fig. 4.2.1 and 4.2.2). For the junction with a length of 150 nm, there is Josephson effect at 2.1 K (red curve in Fig. 4.2.1), but when the temperature is increased to 3.1 K, this effect is lost (red curve in Fig. 4.2.3). We have to go to a much smaller junction, $l = 75$ nm, in order to see a Josephson effect at the two temperatures, 2.4 K (black curve in Fig. 4.2.1) and 3.1 K (black curve in Fig. 4.2.2). The measured normal resistances are slightly higher at 3.1 K than at 2.4 K (Fig. 4.2.3), as in a normal metal the increase in temperature implies an increase in the normal resistance.

The critical currents of the Nb-Cu/Co-Nb junctions as a function of the length are plotted in Fig. 4.2.4. Moreover, in order to see the difference between the critical current of the Nb-Cu/Co-Nb and Nb-Cu-Nb, Fig 4.2.5 summarizes the $I_{c,jj}$-s of these two types of junctions at temperatures of 2.4 K and 3.1 K. It can clearly be seen how the critical currents of the S-N/F-S junctions are suppressed, meaning that when placing 10 nm of Cobalt next to the 50 nm layer of copper, the critical currents become much lower.

If we analyze the values of the I_c of the junctions with 150 nm, JJ.N2.150 and JJ.NF.150, we see that at $T = 2.4$ K the I_c is reduced from 325 μA(Nb-Cu-Nb), to 13.35 μA (Nb-Cu/Co-Nb); and at $T = 3.1$ K, the I_c is reduced from 98.85 μA(Nb-Cu-Nb) to zero(Nb-Cu/Co-Nb).

In S-N/F-S junctions, the normal metal is not only affected by the prox-

imity effect induced due to the superconductors, but also by the ferromagnet which is placed next to it. This ferromagnet tries to allign the spins of the Cooper pairs, making them break faster, meaning a smaller critical current of the junctions and even the complete suppression of the Josephson effect for some of them.

Our results are in agreement with the ones of T.E. Golikova, et. al., who easured Al-(Cu/Fe)-Al bridges(Fig. 5.2.1).

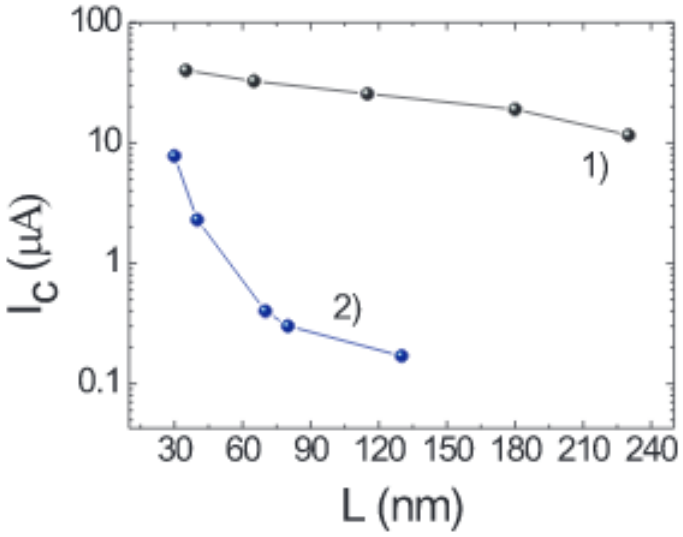

Fig 5.2.1. Dependences of the critical current I_c on the sample length L for (1)Al-Cu-Al and (2) Al-(Cu/Fe)-Al nanobridges at T=0.4 K. This figure is taken from reference [2].

It must be underlined the surprising influence that such a thin layer of Cobalt (5 times smaller than the one of the Copper) has in the normal metal. The exchange interaction of the cobalt, which is the responsible for the pair breaking, affects strongly in the proximity effect induced into the normal metal, even if we could expect that the Cu layer is thick enough to be considered independent from the Co layer. In the weak link, the coupling of the electrons is not due to electro-phonon interactions characteristic of Cooper

pair, but to the relation of the electron and the reflected hole. This superconducting coupling has a length scale bigger than the coherence length. The coherence length is related to the size of the Cooper pairs and in the case of niobium, has a value of around 7 nm. The length scale that characterizes the superconducting correlations in the normal metal is comparable or even bigger than the thickness of the NF bilayer, which drives us to the conclusion that the 2 layers (Cu and Co) cannot be considered as two parallel channels independent from each other, but as whole. This would explain why the superconducting correlations can be affected by the exchange interaction of the ferromagnet.

The results showed in this thesis shed a bit more light on the phenomenon of Andreev reflection and provide us with a slightly better understanding of it. This also leads to more interesting and unanswered questions about this phenomenon. It would be interesting to perform further experiments which could allow us to know at which thickness of the Cu layer the superconducting correlations stop being affected by the exchange interaction, or, at the same time, which thickness of the Co layer is small enough to avoid the effect of this interaction.

Chapter 6

Conclusion

In this thesis it has been analyzed how strongly a ferromagnet influences the proximity effect which is induced into the normal metal of a weak link. Firstly, planar S-N-S Josephson junctions have been characterized. We have analysed Nb-Cu-Nb structures, with thicknesses of 50 nm in both the Nb and Cu layers. The values of the critical currents for gap lengths of 150 nm and 300 nm have been measured, and their temperature dependence has also been studied. The short gap clearly shows a bigger critical current than the larger one, meaning that the superconducting correlations are stronger as the gap length is reduced. Furthermore, we have realized how strongly the temperature affects the Josephson effect. With the study of the temperature dependence, an estimation of the Thouless energy of our junctions has been made. Our Josephson junctions are not in the long junction limit regime, but they show a consistent temperature and gap length dependence. Moreover, our structures are repeatable and reproducible which drives us to the conclusion that our Nb-Cu-Nb junctions are reliable to work with. As a next step, a thin layer (10 nm) of Co has been placed next to the normal metal, thus creating planar S-N/F-S Josephson junctions. The critical current of these junctions has been analyzed for two different temperatures, 2.4 K and 3.1 K. Surprisingly, the values of the critical currents are remarkably much lower than the ones measured with the S-N-S junctions. For the junction with 150 nm gap length, at 2.4 K the Ic is suppressed by a factor of 25 due to the effect of the ferromagnet. At 3.1 K, gap lengths above, and including, 150 nm, show a finite resistance along all the range of the current, meaning that the Josephson effect is completely suppressed, while in S-N-S junctions gap lengths of 150 nm and 300 nm show a supercurrent at temperatures up

to 3.5 K-4 K.

We would like to remark the strong effect of the ferromagnetic exchange interaction on the weak link, which is 50 nm thick. We believe that the reason for this is that the superconducting coupling of the electrons and the reflected holes in the normal metal is affected by the pair breaking interaction because the length scale is comparable to or even bigger than the thickness of the Cu/Co bilayer. Hence, the layer of the normal metal and the layer of the ferromagnet cannot be considered independent from each other, but as a whole. This means that the length scale of the superconducting correlation explores the whole bilayer.

The results of this thesis drives us to the final conclusion that the critical current of the Josephson junctions is dramatically supressed when placing a thin layer of ferromagnet next to a normal metal due to the non-locality of the superconducting correlations.

Chapter 7

Appendix

The method we use for the fabrication of our devices implies the lift off procedure and positive resists. We clearly notice that the main disadvantage of this procedure is the decrease in the critical temperature of our superconductor. In order to protect the Niobium from the degasing of the resist and therefore, raise the Tc to obtain more reliable measurements, we sputter a thin layer of Cupper on top our structure.

In this appendix we give the steps taken for the fabrication of the Josephson junctions.

Method

1st step: Cut a sample of silicon substrate with an area around 5 mm x 5 mm. Clean it with demi water, acetone and isopropanol.

2nd stp: E-beam litography using a positive resist. We deposit two layers of positive reists: the first one is AR-P 662.06 PMMA 600 K and the second layers is AR-P 672045 PMMA 950 K. The positive resist will not protect the structure we make with the e-beam: it changes the chemical structure of the resist so that it becomes more soluble in the developer. The exposed resist is then washed away by the developer solution.

For making the pattern in the e-beam, we use dose of 250 $\mu V/m$ and PC 1 for the contacts and dose 450 $\mu V/m$ and PC 10 for the smallest features of the pattern, such as the global marks or the bridge of the junction.

3rd step: Sputtering materials with the ATC-1800 sputtering system. We use Argon plasma and a sputtering presure of 5.2 Torr. The background presure of teh chamber before sputtering is about $5 - 15 \times 10^{-8}$ mBar

Suttering time:

- 7 nm of Cu: 1 minute and 40 seconds.

-50 nm of Nb: 10 minutes and 25 seconds.

-50 nm of Cu: 16 minutes and 5 seconds.

-10 nm of Co: 5 minutes and 27 seconds. (for the fabrication of S-N/F-S junction)

We may note that sputtering 10 minutes of Nb before inserting the samples lows the base presure of the chamber improving the properties of the Nb in our structures: the Tc of Nb increases half a kelvin.

4rd step: We clean our substrate with acetone to remove the resist, and at the same time, the Nb and Cu which is around the structure.

5th step: We deposit a different positive resist on top. We use the resist called AR-P 6200/2. We make the josephson junction using the e-beam. Making use of the allignment procedures and the global and writting field marks we have made in our structure, we make the gap.

The dose used for these very small gaps (75-300 nm length) is around 150 $\mu V/m$, and PC 12.

We clean our substrate with acetone to remove the resist which is on top.

6th step: We etch the thin layer of Cu on top using the Ion Beam etcher,at an etching presure around 310^{-4} mBar. For 5 nm of Cu the etching time is 45 seconds. We also remove the 50 nm of Nb which is on top of the gap using Plasma etching, using CF4 gas flow of 30 sccm, O2 gas flow of 4 sccm and RF forwrd power of 100 watt. The etching time in this case, is 2 minutes and 20 seconds.

7th step: We clean our sample using the remover for this particular resist: AR-300-70 (NEP).

8th step: We can check the gap using the Scanning Electron Microscope (SEM)

Chapter 8

References

[1] Josephson, B. D., 'Possible new effects in superconductive tunnelling', Physics Letters 1, 251 (1962)

[2] T.E. Golikova, F.H*ü*bler, D.Beckmann, I.E.Batov, T. Yu. Karminskaya, M. Yu. Kupriyanov, A.A. Golubov, and V.V. Ryazanov, 'Double proximity effect in hybrid planar superconductor-(normal metal/ferromagnet)-superconductor structures', Phys.Rev. B 86, 064416 (2012)

[3]Meissner, W.; R. Ochsenfeld. 'Ein neuer Effekt bei Eintritt der Supraleitfhigkeit'. Naturwissenschaften 21 (44): 787788. (1933)

[4] James F.Annet, 'Superconductivity, Superfluids and Condensates',(2004)

[5] V.V. Schmidt, Paul Mller, Alexey V. Ustinov, 'The Physics of Superconductors', (1982)

[6] Bascom S. Deaver, Jr. and William M. Fairbank, 'Experimental Evidence for Quantized Flux in Superconducting Cylinders',Phy. Rev. Lett. 7, 43 (1991)

[7] Shane A.Cybart, Dissertation: 'Planar Josephson Junctions and arrays in by Electron Beam litography and Ion damage' (2005).

[8] Bardeen, J.Cooper, L.N. Schriefffer, J.R., 'Microscopic theory of superconductivity', Phys. Rev. 106, 162 (1957).

[9] Ruur Keizer, PhD Thesis: 'Singlet and triplet supercurrents' (2007)

[10] D.A. Dikin, M. Mehta, C.W. Bark, C.M. Folkman, C.B. Eom, V. Chandrasekhar, 'Coexistence of Superconductivity and Ferromagnetism in Two Dimensions' (2011)

[11] A. Singh, S. Voltan, K. Lahabi, and J. Aarts, 'Colossal Proximity Effect in a Superconducting Triplet Spin Valve Based on the Half-Metallic Ferromagnet CrO2', Phys. Rev. X 5, 021019 (2015)

[12] Y.V. Fominov, A.A. Golubov, T.Y. Karminskaya, M.Y. Kupriyanov, R.G. Deminov, and L.R. Tagirov, 'Superconducting Triplet Spin Valve', JETP Lett. 91, 308 (2010)

[13] H. Courtois, M. Meschke, J. T. Peltonen, and J. P. Pekola, 'Origin of Hysteresis in a Proximity Josephson Junction', PRL 101, 067002 (2008).

[14] B. Pannetier and H. Courtois, 'Andreev Reflection and Proximity effect' (1999)

[15] P. Dubos, H. Courtois, P. Pannetier. ' The Josephson critical current in a long mesoscopic S-N-S junction' (2001).